Enhancing associative learning in rats with a computationally designed training protocol

Xu O. Zhang; Yili Zhang; Claire E. Cho; Douglas S. Engelke; Paul Smolen; John H Byrne; Fabricio H. Do-Monte[#].

Department of Neurobiology and Anatomy, McGovern Medical School, The University of Texas Health Science Center at Houston, Houston, Texas 77030

#Corresponding author:

Fabricio H. Do Monte, DVM, PhD.

Phone: 713-500-5613

Email: fabricio.h.domonte@uth.tmc.edu

Abbreviated title: Enhancing learning with a computational model

Number of pages: 55 pages

Number of figures: 7 Figures

Words: Abstract (231 words), Introduction (728 words), Discussion (1510 words)

Conflict of Interests: The authors declare no competing financial interests.

Acknowledgments: This work was supported by the Russell and Diana Hawkins Family Foundation Discovery Fellowship and the Dr. John J. Kopchick Fellowship to X.O.Z, NIH grant R01-NS102490 to J.H.B, and NIH grant R00-MH105549, NIH grant R01-MH120136, a Brain & Behavior Research Foundation grant (NARSAD Young Investigator), and a Rising STARs Award from UT System to F.H.D-M. We thank Nikita Watson and Sharon Gordon for their technical and administrative assistance. We also thank current members of the Byrne and Do Monte labs for their valuable comments on the manuscript.

Abstract

Associative learning requires the activation of protein kinases with distinct temporal dynamics. Learning protocols with computationally designed intertrial intervals (ITIs) that maximize the interaction between fast-activated protein kinase A (PKA) and slow-activated extracellular signal-regulated kinase (ERK) enhance nonassociative learning in *Aplysia*. Here, we tested whether an optimal learning protocol with irregular ITIs, predicted computationally to increase the overlap between PKA and ERK signaling in rat hippocampus, would enhance associative learning in mammals. We simulated ~1000 training protocols with irregular ITIs to identify this optimal protocol, predicted to induce stronger associative learning than standard protocols with fixed ITIs. With auditory fear conditioning, we showed that male adult rats exposed to the optimal conditioning protocol exhibited stronger fear memory retrieval and impaired fear memory extinction, compared to rats that received either massed or spaced conditioning protocols with fixed ITIs. With fear extinction, we likewise observed that fear conditioned rats exposed to the optimal extinction protocol showed improved extinction of contextual fear memory, compared to rats that received standard extinction protocols. Immunohistochemical staining confirmed that the optimal conditioning protocol increased phosphorylated cAMP responsive element binding (pCREB) protein levels in the dentate gyrus (DG) of the dorsal hippocampus. These findings demonstrate the capacity of a behavioral intervention driven by a computational model of memory-related signaling pathways to enhance associative learning in mammals, and may provide greater insight into strategies to improve cognition in humans.

Keywords: Associative memory, fear conditioning, fear extinction, long-term potentiation, learning model, spaced learning.

Significance Statement

To test if associative learning in mammals can be enhanced by predetermined training protocols, we used a computational model of the dynamics of essential biochemical cascades for learning and memory to predict an optimal training protocol in rats. Using auditory fear conditioning and fear extinction tests, we demonstrated that the optimal protocol enhanced the acquisition and the extinction of fear memories. Immunostaining confirmed that the optimal protocol induced greater levels of pCREB in rat hippocampus. Our results suggest that a non-invasive behavioral intervention guided by computational modeling can be used to enhance associative learning in mammals, with potential relevance for facilitating memory formation as well as enhancing extinction-based therapies in humans.

63 **INTRODUCTION**

64 Long-term memory (LTM) formation that lasts for days to years is believed to be mediated
65 by synaptic plasticity including long-term potentiation (LTP) or its invertebrate analogue
66 long-term facilitation (LTF), which require gene expression and protein synthesis (Martin
67 et al., 2000; Kandel, 2001; Lynch, 2004; Alberini, 2009; Byrne and Hawkins, 2015).
68 Studies in the last decades have investigated LTP/LTF and their underlying molecular
69 processes as potential targets to enhance learning or restore memory deficits in
70 laboratory animals. However, traditional interventions using systemic cognitive enhancers
71 or intracerebral pharmacological manipulations (Sharif et al., 2021; Lauterborn et al.,
72 2016; McGaugh and Petrinovich, 1965; Lynch et al., 2014; Fernandez et al., 2008) are
73 either based on trial-and-error approaches in specific model systems or are highly
74 invasive, making the translation of such interventions difficult for human applications. The
75 recent development of neural recording and optogenetic techniques has enabled precise
76 control of neurons based on their intrinsic firing rates in order to enhance learning or
77 modify memories (Brown et al., 2012; Nabavi et al., 2014; Lee et al., 2017; Liu et al.,
78 2012), but the use of these techniques in humans remains unforeseeable in the near
79 future.

80

81 An alternative approach to enhance learning and memory is to develop computational
82 models to predict optimal training protocols based on the intracellular molecular cascades
83 that underlie LTM formation and LTP/LTF induction (Smolen et al., 2016; Smolen et al.,
84 2020; Zhang et al., 2021). Previous studies have identified activation of PKA (Schacher
85 et al., 1988; Goldsmith and Abrams, 1991; Muller and Carew, 1998) and of the mitogen-

activated protein kinase (MAPK) isoform ERK (Martin et al., 1997; Sharma and Carew, 2004; Sharma et al., 2003) as essential cascades for LTF. These two pathways converge to phosphorylate transcriptional factors such as CREB, which subsequently induce expression of multiple plasticity-related genes (Dash et al., 1990; Bartsch et al., 1995; Liu et al., 2011). The observation that that these two pathways exhibit distinct kinetics of activation (Muller and Carew, 1998; Philips et al., 2007; Zhang et al., 2021), suggests that the temporal activity patterns, and activation overlap, of these pathways may constitute an important target to enhance associative learning. Accordingly, our previous study demonstrated that a computationally designed protocol with irregular ITIs predicted to maximize the overlap of PKA and ERK activities enhances LTF and nonassociative learning, specifically the long-term sensitization of the tail elicited siphon-withdrawal reflex in *Aplysia* (Zhang et al., 2011).

Substantial similarities between molecular processes of LTF in invertebrates and LTP in mammals make it plausible that the same strategies used to enhance LTF and nonassociative learning in invertebrates could enhance LTP and associative learning in mammals. PKA activation in rodent hippocampus and amygdala is required for LTP and LTM (Schafe and LeDoux, 2000; Abel et al., 1997). Similarly, activation of ERK/MAPK cascades and their cross-talk with PKA kinase are required for the phosphorylation of CREB and LTP induction (Adams and Sweatt, 2002; Impey et al., 1998). Albeit with different kinetics than observed in invertebrates, PKA and ERK activation in mammals also differ considerably in temporal dynamics (Roberson and Sweatt, 1996; Vázquez et

al., 2000; Wang et al., 2014), providing a similar opportunity to maximize their overlap with irregular ITIs in an attempt to enhance memory formation.

Here, we tested if the invertebrate LTF model (Zhang et al., 2011) can be adapted to computationally design an optimal associative learning protocol in mammals. Empirical data from the literature were used to model PKA and ERK dynamics in rat hippocampus (Wang et al., 2014; Roberson and Sweatt, 1996; Vázquez et al., 2000), a critical brain region implicated in the formation of associative memories in mammals (Milner et al., 1998; Mayes et al., 2007; Nakazawa et al., 2002). Then we simulated ~1000 different training protocols with irregular ITIs and identified an optimal protocol, predicted to induce stronger memory than standard training protocols with fixed ITIs. Using auditory fear conditioning and fear extinction paradigms in rats, we demonstrated that our computationally designed protocol enhanced the acquisition as well as the extinction of fear memories. Using immunohistochemical staining, we confirmed that the computationally designed protocol induced greater levels of pCREB in the DG of the dorsal hippocampus. This strategy may have potential clinical relevance for interventions aiming at facilitating memory formation in psychiatric disorders associated with cognitive impairment in humans, as well as to enhance extinction-based therapies in patients suffering from fear-related disorders.

131 **MATERIALS AND METHODS**

132 **Animals**

133 All experimental procedures were approved by the Center for Laboratory Animal Medicine
134 and Care of The University of Texas Health Science Center at Houston. National
135 Institutes of Health guidelines for the care and use of laboratory animals were strictly
136 followed in order to minimize any potential discomfort and suffering. A total of 120 male
137 Long-Evans hooded adult rats (Charles Rivers Laboratories) 3-5 months of age and
138 weighing 330-450 g were used. Rats were kept in a 12-hour light/12-hour dark cycle with
139 food and water *ad libitum*. Experiments were conducted during the light phase. For the
140 Optimal Extinction experiment, animals were maintained on a restricted diet of 18 g per
141 day of standard laboratory rat chow to increase their motivation during the lever press
142 training. Rats' weights were monitored weekly to make sure that all animals maintained
143 their weight under food restriction.

144

145 **Model Development**

146 The mathematical model for the activation of kinase cascades critical for long-term
147 memory (LTM) was modified from a previous model of the signaling cascades for the
148 induction of long-term synaptic facilitation (Zhang et al., 2011). As mentioned above, the
149 induction of LTM for fear conditioning is known for requiring the activation of multiple
150 kinase cascades with different temporal dynamics. In the model, the cyclic AMP (cAMP)-
151 PKA pathway is rapidly activated after training, whereas the Raf- MEK-ERK pathway is
152 slowly activated, and both are required for the induction of LTM after fear conditioning
153 and extinction (**Fig. 1A, Fig. 4A**).

154 *PKA Pathway.* The dynamics of cAMP activation upstream of PKA following
155 training and the cAMP-dependent activation of PKA are described by Eqs. 1-4. Inactive
156 PKA is a holoenzyme (PKA_{RC}, Eq. 2), consisting of regulatory (PKA_R, Eq. 3) and catalytic
157 (PKA_C, Eq. 4) subunits. In response to training, represented by the variable *Stim* in Eq.
158 1, cAMP is activated (Eq. 1). Active cAMP binds to the regulatory subunit of PKA, leading
159 to the release of free, active catalytic subunit (Fig. 1A) (Eqs. 2-4). '*Stim*' represents the
160 neurotransmitters released by training that function to activate kinase cascades.

161

162 $$\frac{d[cAMP]}{dt} = \lambda \frac{[Stim]}{[Stim] + K_{Stim}} - k_{b,cAMP}[cAMP] \quad \text{(Eq. 1)}$$

163 $$\frac{d[PKA_{RC}]}{dt} = k_{b,PKA}[PKA_C][PKA_R] - k_{f,PKA}[PKA_{RC}][cAMP]^2 \quad \text{(Eq. 2)}$$

164 $$\frac{d[PKA_R]}{dt} = k_{f,PKA}[PKA_{RC}][cAMP]^2 - k_{b,PKA}[PKA_C][PKA_R] \quad \text{(Eq. 3)}$$

165 $$\frac{d[PKA_C]}{dt} = k_{f,PKA}[PKA_{RC}][cAMP]^2 - k_{b,PKA}[PKA_C][PKA_R] \quad \text{(Eq. 4)}$$

166

167 Parameter values are modified from (Zhang et al., 2011) to activate PKA immediately
168 after training, but with PKA activity quickly returning to the basal in ~5 min (Fig. 1B)
169 (Roberson and Sweatt, 1996; Vázquez et al., 2000): λ = 14.6 μM/min, K_{STIM} = 85 μM,
170 $k_{b,cAMP}$ = 4 min^{-1}, $k_{f,PKA}$ = 20 $\mu M^{-2} min^{-1}$, $k_{b,PKA}$ = 12 $\mu M^{-1} min^{-1}$

171

172 *ERK Pathway.* The activation of ERK by training '*Stim*' is via sequential activation
173 of the upstream kinases Raf and MEK (Fig. 1A). Raf activates the MAP kinase kinase

174 MEK, MEK in turn activates the MAP kinase ERK. The differential equations describing
175 the activation of Raf, MEK, and ERK (Eqs. 5-12) are similar to those in (Zhang et al.,
176 2011). However, a discrete time delay in activation of Raf was removed from the
177 phosphorylation of Raf (Eq. 5). Instead, based on empirical data (Wang et al., 2014; Ajay
178 and Bhalla, 2004), parameters describing the activation of Raf were adjusted from (Zhang
179 et al., 2011) so that the ERK activation curve reached the peak around 20 min post-
180 training (Fig. 1B).
181

182 $$\frac{d[Raf^p]}{dt} = k_{f,Raf}[Raf][Stim] - k_{b,Raf}[Raf^p] \quad \text{(Eq. 5)}$$

183 $$[Raf] = [Raf]_{total} - [Raf^p] \quad \text{(Eq. 6)}$$

184 $$\frac{d[MEK]}{dt} = \frac{k_{b,MEK}[MEK^p]}{[MEK^p] + K_{MEK,2}} - \frac{k_{f,MEK}[Raf^p][MEK]}{[MEK] + K_{MEK,1}} \quad \text{(Eq. 7)}$$

185 $$\frac{d[MEK^{pp}]}{dt} = \frac{k_{f,MEK}[Raf^p][MEK^p]}{[MEK^p] + K_{MEK,1}} - \frac{k_{b,MEK}[MEK^{pp}]}{[MEK^{pp}] + K_{MEK,2}} \quad \text{(Eq. 8)}$$

186 $$[MEK^p] = [MEK]_{total} - [MEK] - [MEK^{pp}] \quad \text{(Eq. 9)}$$

187 $$\frac{d[ERK]}{dt} = \frac{k_{b,ERK}[ERK^p]}{[ERK^p] + K_{ERK,2}} - \frac{k_{f,ERK}[MEK^{pp}][ERK]}{[ERK] + K_{ERK,1}} \quad \text{(Eq. 10)}$$

188 $$\frac{d[ERK^{pp}]}{dt} = \frac{k_{f,ERK}[MEK^{pp}][ERK^{p}]}{[ERK^{p}] + K_{ERK,1}} - \frac{k_{b,ERK}[ERK^{pp}]}{[ERK^{pp}] + K_{ERK,2}} \quad \text{(Eq. 11)}$$

189 $$[ERK^{p}] = [ERK]_{total} - [ERK] - [ERK^{pp}] \quad \text{(Eq. 12)}$$

190 Parameter values: $k_{f,Raf}$ = 0.001 μM^{-1}min^{-1}, $k_{b,Raf}$ = 0.05 min^{-1}, $[Raf]_{total}$ = 0.5 μM,

191 $k_{f,MEK}$ = 0.41 min^{-1}, $k_{b,MEK}$ = 0.04 μM/min, $K_{MEK,1}$ = 0.20 μM,

192 $K_{MEK,2}$ = 0.19 μM, $[MEK]_{total}$ = 0.5 μM, $k_{f,ERK}$ = 0.41 min^{-1},

193 $k_{b,ERK}$ = 0.12 μM/min, $K_{ERK,1}$ = 0.19 μM,

194 $K_{ERK,2}$ = 0.21 μM, $[ERK]_{total}$ = 0.5 μM.

195 As in (Zhang et al., 2011), a variable '*inducer*' was used to quantify the overlap of

196 activation between PKA and ERK, which together regulate the gene expression

197 necessary for the induction of LTM.

198 $$inducer = k_{inducer}\,[PKA_C]\,[ERK^{pp}] \quad \text{(Eq. 13)}$$

199 where $k_{inducer}$ = 1 μM^{-1}.

200 To determine which protocols could more effectively activate *inducer,* four-trial protocols

201 with three ITIs, each ranging from 2–20 min in steps of 2 min, were simulated. Combining

202 these permutations yielded 10^3 protocols. For each protocol, the maximal (peak) overlap

203 between PKA and ERK was quantified as the peak level of *inducer* produced. Also, the

204 value of *Stim* was varied from 100 to 300 μM to represent weak and strong trainings and

205 to test the robustness of protocols. Based on the maximal overlap, a protocol with ITIs of

206 8, 8, and 16 min was selected and was denoted optimal partial conditioning (OPC). We

207 assumed that fear conditioning and extinction activate the same signaling pathways, so
208 we predicted this protocol would similarly enhance extinction.

209 *Numerical methods.* Fourth-order Runge-Kutta integration was used for
210 integration of all differential equations with a time step of 3 s. Further time step reduction
211 did not lead to significant improvement in accuracy. The steady-state levels of variables
212 were determined after at least one simulated day, prior to any manipulations. The model
213 was programmed in XPPAUT (http://www.math.pitt.edu/~bard/xpp/xpp.html) (Ermentrout,
214 2002) and simulated on Dell Precision T1700 microcomputers.

215

216 **Behavioral Tasks**

217 ***Optimal Conditioning***

218 *Apparatuses*

219 Two distinct chambers (context A and context B) positioned inside sound attenuating
220 boxes were used during the Optimal Conditioning experiments. Context A consisted of a
221 small operant chamber (34 cm high x 25 cm wide x 23 cm deep, 200 lux, Med Associates,
222 see schematic drawing in Fig. 2A top) with one of the two aluminum walls covered by
223 black adhesive paper and two transparent acrylic walls, and a metal grid floor beneath
224 which a microcentrifuge tube (Eppendorf) containing 50 µl of 10% amyl acetate (Sigma-
225 Aldrich) was positioned. Context B consisted of a larger acrylic operant chamber (40 cm
226 high x 50 cm wide x 26 cm deep, 20 lux, Med Associates, see schematic drawing in Fig.
227 2A bottom) with one of its walls covered by a black and white stripped paper, and a floor
228 made of a white acrylic board beneath which a microcentrifuge tube (Eppendorf)
229 containing 50 µl of deionized water was positioned.

230

231 *Procedures*

232 On day 0, rats were placed in context A for a 20-min familiarization session. Next, rats
233 were assigned to three experimental groups by matching their baseline freezing and
234 locomotor activity during the familiarization session: Full Conditioning (FC), Partial
235 Conditioning (PC), and Optimal Partial Conditioning (OPC). On day 1, rats were placed
236 into context A and exposed to one nonreinforced habituation tone (3 kHz, 75 dB, 30 s)
237 followed by distinct fear conditioning protocols (44 min duration). The FC group received
238 eight presentations of a conditioned stimulus (CS, 3 kHz tone, 75 dB, 30 s) that co-
239 terminated with an unconditioned stimulus (US, footshock, 0.7 mA, 0.5 s), with fixed ITIs
240 of 270 s. The PC group received four similar CS-US pairings with the same ITIs of 270 s,
241 and remained in the chamber until the end of the session. The OPC group received four
242 similar CS-US pairings with ITIs of 8, 8, and 16 min. On day 2, rats were placed in context
243 B and given two CS presentations (ITI of 150 s, 7 min duration) in the absence of US to
244 test the retrieval of tone-associated fear memory in a novel context. On day 3, rats were
245 returned to context A for an extinction training session where they received twelve CS
246 presentations (ITIs of 150 s, 37 min duration). The first four CSs were compared to the
247 last four CSs to assess extinction learning within the same session. On day 4 and 5, rats
248 were placed back in context A and B, respectively, and exposed to an extinction retrieval
249 session (similar to day 2). On day 29 and 30, rats were placed back in context A and B,
250 respectively, and exposed to a spontaneous recovery session (similar to day 2). On day
251 1 and day 2, rats in the same group were trained simultaneously in four chambers with
252 the group order counterbalanced to avoid interference from different protocols in

253 neighboring chambers. On the following days, rats were simultaneously tested in four
254 chambers regardless of the group assignment. Each rat was tested in the exact same
255 chamber across the days. Footshocks, tones, intertrial intervals, and session duration
256 were controlled by an automated video tracking system (ANY-maze, Stoelting), which
257 also quantified the percentage of time freezing, distance traveled, average speed and
258 maximum speed. All rats passed the criteria of 20% of freezing during at least one CS of
259 the fear conditioning session and the first two CSs of the extinction session.
260
261 ***Optimal vs. Spaced Partial Conditioning***
262 *Apparatus and Procedures*
263 The same apparatus and contexts described above were used. Following familiarization
264 on Day 0, rats were assigned to two experimental groups by matching their baseline
265 freezing and locomotor activity during the familiarization session: Optimal Partial
266 Conditioning (OPC) and Spaced Partial Conditioning (SPC). The same procedures
267 described above were used here, except that: *i)* the footshock intensity was reduced from
268 0.7 mA to 0.5 mA to decrease the possibility of ceiling effects; *ii)* the SPC group received
269 four CS-US pairings with ITIs of 11 min and 10 s. The same automated video tracking
270 system (ANY-maze, Stoelting) described above was used for protocol control and
271 behavioral quantification. One rat that failed the criteria of 20% of freezing during at least
272 one CS of the fear conditioning session and the first two CSs of the extinction session
273 was excluded from the analyses.
274
275

276 ***Optimal Extinction***

277 *Lever-press training*

278 Rats were placed in an acrylic/aluminum operant chamber (34 cm high x 25 cm wide x
279 23 cm deep, Med Associates, see schematic drawing in Fig. 4A) and trained to press a
280 lever for sucrose on a fixed ratio of one pellet for each press. Next, animals were trained
281 in a variable interval schedule of reinforcement that was gradually reduced across the
282 days (one pellet every 15 s, 30 s, or 60 s) until they reached a minimum criterion of 10
283 presses/min after 7 days of training. All sessions lasted 30 min and were performed on
284 consecutive days. Sucrose pellet delivery, variable intervals, and session duration were
285 controlled by an automated video tracking system (ANY-maze, Stoelting).

286

287 *Apparatus and Procedure*

288 On day 8, rats were placed into the same chamber where they had previously undergone
289 lever presses training. Animals were exposed to five nonreinforced habituation tones (3
290 kHZ, 75 dB, 30 s duration) followed by seven CS-US pairings (ITIs of 150 s, 37 min
291 duration). The footshock intensity was increased from 0.7 mA to 1.0-1.2 mA to result in
292 stronger fear acquisition and consequently higher freezing levels during the extinction
293 training session in the next day. Rats were assigned to three experimental groups by
294 matching their freezing and lever presses during the fear conditioning session: Full
295 Extinction (FE), Partial Extinction (PE), and Optimized Partial Extinction (OPE). On day
296 9, rats were returned to the same chamber for a fear extinction session (39 min duration).
297 The FE group received twelve CSs with ITIs of 150 s; the PE group received four CSs
298 with ITIs of 150 s and remained in the chamber until the end of the session; and the OPE

299 group received four CSs with ITIs of 8, 8, and 16 min. On day 10 and 35, rats were placed
300 into the same chamber and received two CSs with an ITI of 150 s to test the strength of
301 fear extinction memory during extinction retrieval and spontaneous recovery tests,
302 respectively. The same automated video tracking system (ANY-maze, Stoelting)
303 described above was used for protocol control and behavioral quantification. Two rats
304 that never reached the criterium of 20% of freezing during at least one CS of the fear
305 conditioning session and the first two CSs of the extinction session were excluded from
306 the analyses.
307
308 **Immunohistochemistry**
309 Rats were perfused with 200 ml of 0.1 M potassium phosphate buffer (KPBS) followed by
310 500 ml of 4% paraformaldehyde (PFA) in 0.1 M sodium phosphate buffer 15 min after day
311 1 of conditioning. Brains were removed from the skull, transferred to a 20% sucrose
312 solution in PFA for 24 h, and stored in a 30% sucrose solution in PFA for another 24 h.
313 Next, coronal brain sections (40 μm thick) were cut with a cryostat (CM1860, Leica) and
314 stored in an antifreeze solution overnight. Sections were blocked in 20% normal goat
315 serum, 0.3% Triton X-100, and 3% hydrogen peroxide in KPBS at room temperature for
316 1 h. Brain sections were then incubated with anti-pCREB serum raised in rabbit (1:1000;
317 EMD Millipore 06-519) overnight at room temperature. After sections were washed with
318 KPBS five times, they were incubated with biotinylated goat anti-rabbit IgG antibody
319 (1:200, Vector Labs, BA-1000-1.5) for 2 h, followed by incubation in ABC kit (1:50, Vector
320 Labs, PK-6100) for 90 min and DAB-Ni solution (Vector Labs, SK-4100) for 25 min.
321 Sections were washed with KPBS and mounted on Superfrost Plus slides. After three

322 days, sections were serially dehydrated with alcohol (Epredia; 50 and 70% for 5min each,
323 95 and 100% for 10 min each) and defatted with Citrisolv (Decon Labs) for 30 min.
324 Sections were then cover-slipped with mounting medium (Permount, Fisher Scientific)
325 before being analyzed microscopically.
326
327 **Microscopy and image analysis**
328 Images were generated with a Nikon microscope (Eclipse NiE Motorized Upright
329 Microscope) equipped with a fluorescent lamp (X-Cite, 120 LED) and a digital camera
330 (Andor Zyla 4.2 PLUS sCMOS). Counts of pCREB-positive cells were performed at 20 x
331 magnification. Cell detection and quantification for the immunohistochemistry experiment
332 were performed automatically using QuPath (Bankhead et al., 2017). pCREB-positive cell
333 detection was performed using QuPath's optical density sum with a requested pixel size
334 of 0.5 µm. Nucleus parameters included a background radius of 6µm, median filter radius
335 of 0 µm, sigma of 1.5 µm, minimum area of 2 μm^2, and maximum area of 250 μm^2. Cell
336 expansion was set to 0 µm. Intensity parameters included a threshold of 0.15 and
337 maximum background intensity of 5, and intensity threshold parameters were threshold
338 1 of 0.2, threshold 2 of 0.4, and threshold 3 of 0.6. pCREB-positive cells were
339 automatically counted with a circular region of interest (0.228 mm^2) in each subfield of rat
340 dorsal hippocampus including CA1, CA2, CA3, and DG according to the Paxinos rat brain
341 atlas (Paxinos and Watson, 2014), and averaged for both hemispheres at 2-3 different
342 antero-posterior levels from -2.4 mm to -4.2 mm from bregma. The density of pCREB-
343 positive cells (cells per mm^2) was calculated by dividing the number of pCREB-positive
344 cells by the area of the circular region of interest.

345 **Quantification and statistical analysis**

346 Rats were recorded with digital video cameras (Logitech C920) and behavioral indices
347 were measured using automated video-tracking system (ANY-maze). Lever presses per
348 minute were calculated by measuring the number of presses during the 30 s cue (or 30 s
349 pre-cue) multiplied by two. All graphics and numerical values reported in the figures are
350 presented as mean ± standard error of the mean (SEM). Grubbs' tests were used to
351 identify outliers ($p < 0.05$) in each experiment and one rat in Fig. 2 was removed after
352 identified by the test. Shapiro-Wilk test were performed to determine whether the data
353 have a normal distribution. F tests before pair-wise comparison and Brown-Forsythe tests
354 before multiple group comparison were performed to test if groups have the same
355 variance. Statistical significance for parametric distributions was determined with paired
356 Student's t-test, Welch's t-test, one-way analysis of variance (ANOVA) or two-way
357 repeated-measures ANOVA followed by Tukey post-hoc comparisons, whereas Kruskal-
358 Wallis test followed by Dunn's post-hoc test was used for non-parametric distributions
359 (Prism 7), as indicated for each experiment. Sample size was based on estimations from
360 previous literature and experience.

361

362 **Data availability**

363 All data that support the findings presented in this study are available from the
364 corresponding author on reasonable request. Source codes will be submitted to the
365 ModelDB database (McDougal et al., 2015), and to GitHub
366 (https://github.com/Owenxz/Zhang-XO-Enhanced-Learning-2022.git).

367

368 **RESULTS**

369 **A computational model based on PKA and ERK dynamics in rats identified an**
370 **optimal partial fear conditioning protocol**

371 The model of (Zhang et al., 2011) was adapted to simulate the dynamics of PKA and ERK
372 during the process of LTP induction in rat hippocampus (**Fig. 1A**). In this model, the
373 stimulus (*Stim*), which represents tetanic stimuli, rapidly activates PKA via the cAMP
374 pathway and slowly activates ERK via the Raf-MEK pathway. The synergistic interaction
375 between PKA and ERK pathways is quantified by a variable *inducer*, which corresponds
376 to the efficacy of the stimulus in inducing LTP. ERK kinetics were described by differential
377 equations (see Methods) with parameter values reproducing empirical findings that ERK
378 activity reaches peak levels 15~20 min after BDNF treatment or tetanic stimuli in rat
379 hippocampus acute slices (Wang et al., 2014; Ajay and Bhalla, 2004). Equations
380 describing PKA kinetics simulated data showing that PKA is transiently activated within 2
381 min after LTP induction in slices from rat hippocampus or within 5 min *in vivo* after spatial
382 discrimination task training (Roberson and Sweatt, 1996; Vázquez et al., 2000). We
383 simulated fear conditioning in rats, in which the pairing of a conditioned stimulus (CS) with
384 an unconditioned stimulus (US) is represented by *Stim*, and the conditioned responses
385 are proportional to the peak value of *inducer*. We observed that a single CS-US pairing
386 produced little overlap between PKA and ERK pathways (**Fig. 1B1**). We then simulated
387 ~1000 partial fear conditioning protocols, with 4 trials and varying ITIs, to identify one
388 predicted to have optimal ITIs for triggering downstream gene activation. To compare, we
389 also simulated a Full Conditioning (FC) protocol with 8 trials and a fixed ITI of 270 s, and
390 a Partial Conditioning (PC) protocol with 4 trials and the same ITI of 270 s, which resemble

391 previous protocols used for full and partial fear conditioning in rats (Detert et al., 2008;
392 Lonsdorf et al., 2017). Our simulation identified an Optimal Partial Conditioning (OPC)
393 protocol with 4 trials and irregular ITIs of 8, 8, and 16 min, which was able to produce
394 higher peak *inducer* than the standard PC protocol with 4 trials (**Fig. 1B2-1B4**).
395 Comparing OPC and PC in Fig. 1B3-B4, both protocols produced pERK curves with
396 similar peak levels (orange). However, PKA activity induced by the last trial of OPC had
397 a much larger overlap with the pERK curve than did PKA induced by PC. Therefore, OPC
398 induced a much higher peak level of *inducer* (purple). We therefore predicted the OPC
399 protocol would produce stronger long-term memory in rats than the standard PC protocol.
400

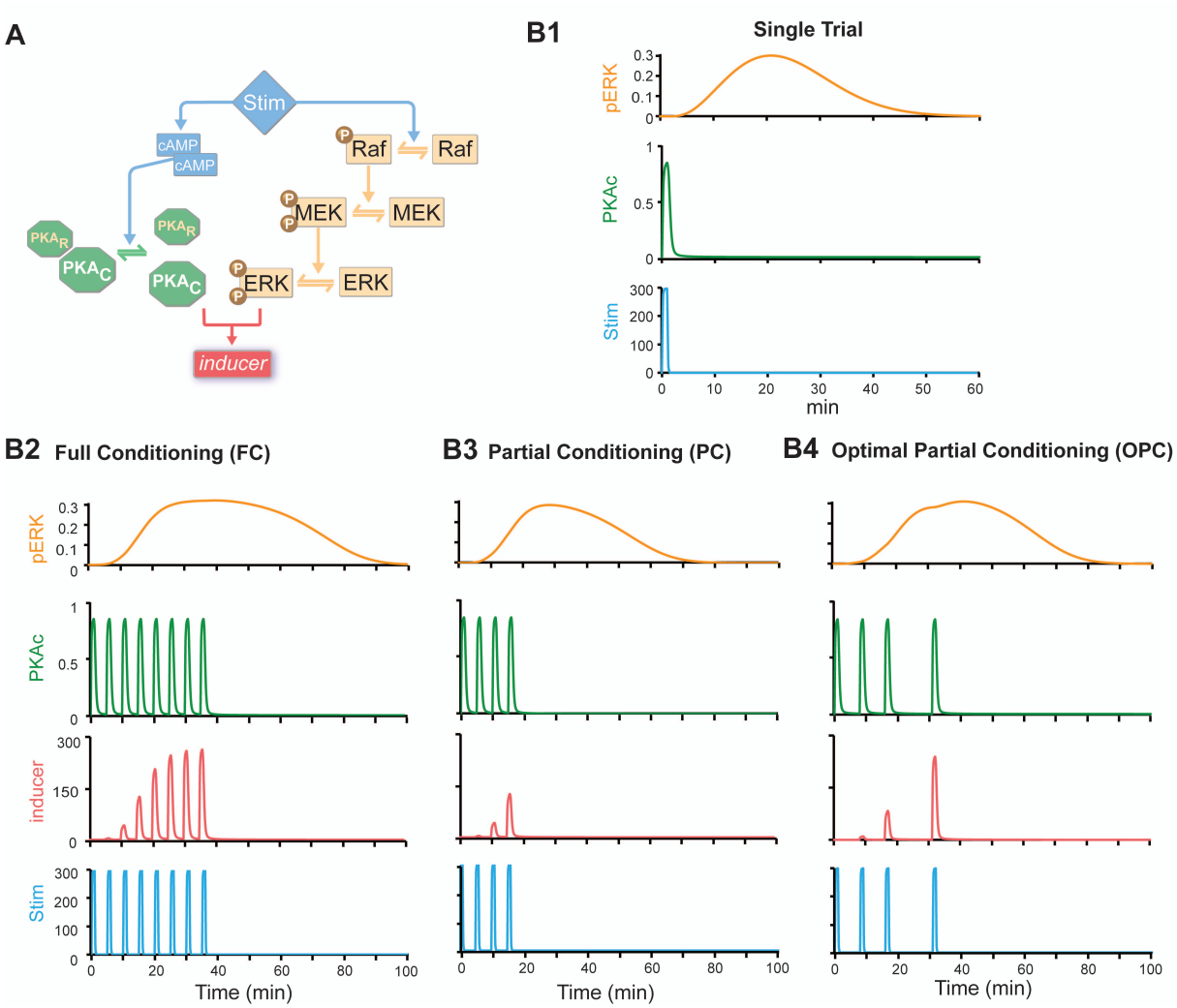

401

402 **Figure 1. Computational simulations of PKA and ERK pathways predict an optimal**

403 **protocol for fear conditioning. A**, Schematic of the model. Stimulus (*Stim*, μM) activates PKA

404 via cAMP and activates ERK via Raf-MEK. The variable *inducer* quantifies the PKA/ERK

405 interaction (activity overlap). **B1**, Simulated time courses of activated ERK (pERK, μM) and

406 activated PKA (PKAc, μM) in response to one trial of *Stim*. **B2**, Simulated time courses of pERK,

407 PKAc, and *inducer* (nM) in response to an 8-trial protocol with regular ITIs of 4.5 min (full

408 conditioning, FC). **B3**, Simulated time courses of pERK, PKAc, and *inducer* in response to a 4-

409 trial protocol with regular ITIs of 4.5 min (partial conditioning, PC). **B4**, Simulated time courses

410 of pERK, PKAc, and *inducer* in response to a 4-trial protocol with computationally designed
411 intervals (optimal partial conditioning, OPC).
412

413 **The optimal partial conditioning protocol induces stronger fear memory than a**
414 **standard partial conditioning protocol**

415 To test if the computationally designed OPC protocol could enhance associative learning
416 in rats, we used a classical auditory fear conditioning paradigm. Because the
417 hippocampus is required for context encoding during fear conditioning (Phillips and
418 LeDoux, 1992; Selden et al., 1991; Maren et al., 2013), we used two different chambers
419 (context A and context B) to assess the contribution of the context to the auditory fear
420 memory. The two contexts differed in size, floor texture, visual decoration of the walls,
421 and odor cues (**Fig. 2A**). On Day 0, rats were pre-exposed to context A for 20 min to
422 familiarize with the chamber where fear conditioning took place in the following day. After
423 matching their baseline freezing and locomotor activity during the familiarization session,
424 rats were assigned to one of the three experimental groups described above in our
425 simulation experiments: Full Conditioning (FC), Partial Conditioning (PC), and Optimal
426 Partial Conditioning (OPC). No significant difference was found among their baseline
427 freezing level (FC: 3.05%, PC: 2.84%, OPC: 2.96%, one-way ANOVA, $F_{(2, 37)} = 0.018$, P
428 $= 0.982$), average speed (FC: 0.023 m/s, PC: 0.025 m/s, OPC: 0.025 m/s, one-way
429 ANOVA, $F_{(2, 37)} = 0.062$, $P = 0.939$), and maximum speed (FC: 0.439 m/s, PC: 0.424 m/s,
430 OPC: 0.446 m/s, one-way ANOVA, $F_{(2, 37)} = 0.044$, $P = 0.956$). On Day 1, rats were placed
431 into context A and exposed to one nonreinforced habituation tone (3 kHZ, 75 dB, 30 s)
432 followed by distinct fear conditioning protocols (44 min duration, **Fig. 2B**). The FC group
433 received eight presentations of CS (3 kHZ tone, 75 dB, 30 s) that co-terminated with an

US (footshock, 0.7 mA, 0.5 s) with ITIs of 270 s. The PC group received four similar CS-US pairings with the same ITIs of 270 s, and remained in the chamber until the end of the session to equate the total context exposure time. The OPC group received four similar CS-US pairings with ITIs of 8, 8, and 16 min. All groups reached high levels of freezing (> 65%, **Fig. 2C**) and reduced locomotion at the end of the fear acquisition session. On Day 2, rats were placed in context B and given two CS presentations (ITI of 150 s, 7 min duration) in the absence of US to test the retrieval of tone-associated fear memory in a novel context. Compared to the FC group, both PC and OPC groups exhibited less freezing during the second CS presentation (Two-way repeated measures (RM) ANOVA followed by Tukey's post-hoc test. $F_{(2, 37)} = 3.751$, $P = 0.033$; FC vs. OPC: p = 0.029; FC vs. PC: p = 0.002; OPC vs. PC: p = 0.527). Nevertheless, both FC and OPC groups showed reduced average speed during the retrieval test compared to the standard PC group, suggesting stronger fear retrieval in a novel context (**Fig. 2D;** One-way ANOVA followed by Tukey's post hoc test. $F_{(2, 37)} = 10.87$, $P < 0.001$; FC vs. OPC: p = 0.131; FC vs. PC: p < 0.001; OPC vs. PC: p = 0.024). On Day 3, rats were returned to context A for an extinction training session where they received twelve CS presentations (ITIs of 150 s, 37 min duration). Although no significant differences in freezing levels were observed among the groups during each CS presentation (Two-way RM ANOVA. $F_{(22, 407)} = 1.169$, $P = 0.271$), a within session extinction analysis comparing the first four CSs to the last four CSs revealed impaired extinction learning in the FC and OPC groups, when compared to the PC group. This impairment in the acquisition of extinction in the FC and OPC groups was characterized by sustained freezing levels across the session, which differed from the PC group that showed reduced freezing levels from the first to the last

457 CSs presentation (**Fig. 2E left;** Paired Student's t-test. FC: t_{13} = 2.153, p = 0.051; PC: t_{11}
458 = 4.191, p = 0.001; OPC: t_{13} = 0.869, p = 0.400**)**. Interestingly, the OPC group exhibited
459 persistent freezing levels during the extinction training session as indicated by a reduced
460 relative change in freezing from the beginning to the end of the session, when compared
461 to the PC group (**Fig. 2E right;** One-way ANOVA followed by Tukey's post-hoc test. $F_{(2,}$
462 $_{37)}$ = 3.315, P = 0.047; FC vs. OPC: p = 0.487; FC vs. PC: p = 0.320; OPC vs. PC: p =
463 0.037). Despite the persistent freezing levels across the extinction training session
464 observed in the OPC group, no significant differences were found between the OPC and
465 the PC groups during either the extinction retrieval tests performed on Days 4 and 5 (Two-
466 way RM ANOVA. context A: $F_{(2, 37)}$ = 0.097, P = 0.907; context B: $F_{(2, 37)}$ = 2.984, P =
467 0.063) or the spontaneous recovery tests performed on Days 29 and 30 (**Fig. 2C;** Two-
468 way RM ANOVA followed by Tukey's post hoc test. context A: $F_{(2, 37)}$ = 3.259, P = 0.049;
469 FC vs. OPC: p = 0.027; FC vs. PC: p = 0.038; OPC vs. PC: p = 0.999; context B: $F_{(2, 37)}$
470 = 0.774, P = 0.469). Taken together, these data demonstrate that the computationally
471 designed OPC protocol is able to enhance fear acquisition in rats, thereby resulting in a
472 stronger fear memory that is more resistant to extinction.

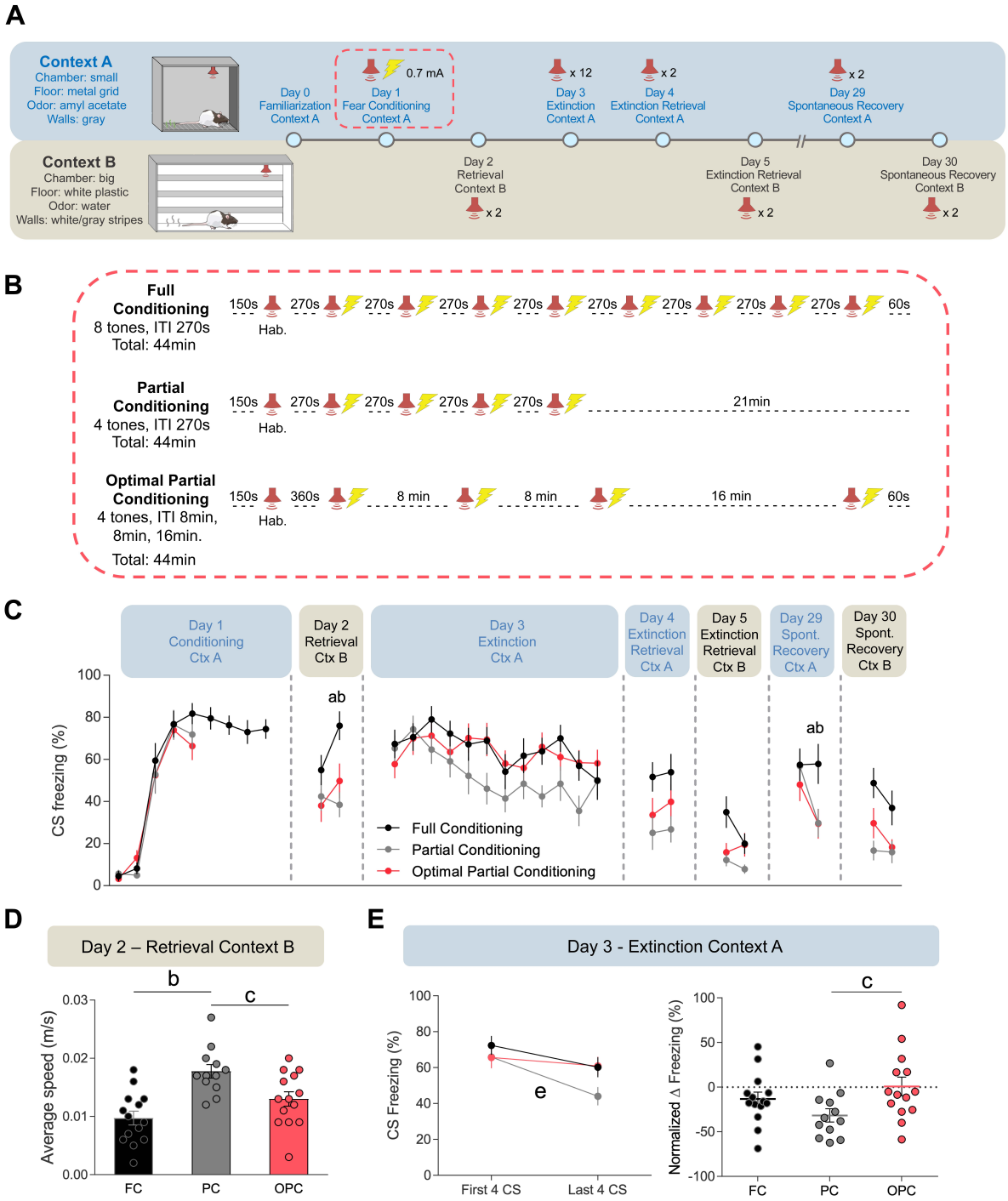

Figure 2. Computationally designed protocol enhanced fear conditioning in rats. **A,** Schematics of the enhanced fear conditioning experimental procedures. Top: tests that were conducted in Context A. Bottom: tests that were conducted in Context B. **B,** Schematics of the

477 fear conditioning protocols for FC (n = 14), PC (n = 12), and OPC (n = 14) groups. Following a
478 habituation (Hab.) tone, rats received multiple trials of a CS (3 kHz tone, 30 s) that co-terminated
479 with a US (footshock, 0.7 mA, 0.5 s). **C,** Freezing levels during CS presentations of each group
480 across the experiment. Two-way Repeated-Measure ANOVA for each day followed by Tukey's
481 post hoc test. Letters a, b, and c indicate pairwise post hoc tests with $p < 0.05$: a, FC vs. OPC; b,
482 FC vs. PC; c, OPC vs. PC. **D,** OPC group shows lower average speed compared to PC group.
483 One-way ANOVA followed by Tukey post hoc test. Letters b and c indicate pairwise tests with p
484 < 0.05: b, FC vs. PC ; c, OPC vs. PC. **E,** OPC group is resistant to extinction while PC group
485 shows significantly more extinction. Left, the freezing levels during the first 4 and last 4 CS
486 presentations. Paired Student's t-test. Letter e indicates test with $p < 0.05$: PC, Last 4 CS vs. First
487 4 CS. Right, normalized change of the freezing level during extinction, as indicated by the
488 difference of the freezing levels between last 4 and first 4 CS presentations as a percentage of
489 the freezing level of the first 4 CS presentations ((Last 4 CS – First 4 CS)/First 4 CS). One-way
490 ANOVA followed by Tukey's post hoc test. * $p<0.05$. Letter c indicates pairwise test with $p < 0.05$:
491 OPC vs. PC. Data shown here and in the next illustrations as mean ± SEM.
492

493 **The optimal partial conditioning protocol induces stronger fear memory than a**
494 **spaced partial conditioning protocol**

495 Previous studies have demonstrated that spaced learning protocols result in stronger
496 memories than standard (i.e., massed) learning protocols in both humans (Cepeda et al.,
497 2006; Raman et al., 2010) and rodents (Anderson et al., 2008; Jiang et al., 2019; Scharf
498 et al., 2002; but also see Cain et al., 2003). Thus, an alternative explanation for the
499 augmented fear memory observed in the OPC group in Fig. 2 could be simply a trial-
500 spacing effect, because our standard PC group used massed CS-US pairings. In
501 simulations, both protocols produced similar peak values of the pERK curves, but different

502 overlap of PKA and ERK activities, suggesting a way in which appropriately spaced
503 protocols might advantageously enhance overlap of kinase activities with distinct
504 dynamics. Indeed, there was a broad range of effective 4-trial protocols (**Fig. 3**), with one
505 protocol with fixed 11 min 10 s ITIs producing a nearly identical peak level of inducer as
506 the OPC protocol, and a higher peak level of inducer than other protocols with fixed ITIs
507 from 1 min to 21 min (**Fig. 3A, Fig. 4A1**). We termed this protocol the spaced partial
508 conditioning (SPC) protocol. We also examined the effects of different stimulus intensities
509 on predicting optimal training trials. The 1,000 different protocols were re-simulated with
510 a reduced intensity of stimulus. Interestingly, the protocol with 4 trials and irregular ITIs
511 of 8, 8, and 16 min still produced the greatest peak level of inducer (**Fig. 3B, Fig. 4A2**).
512 Equally interesting was that with weaker stimuli, the OPC protocol became relatively more
513 effective than the SPC protocol. Therefore, we predicted that empirically, the irregular
514 intervals of the OPC may produce more effective conditioning than the SPC protocol.

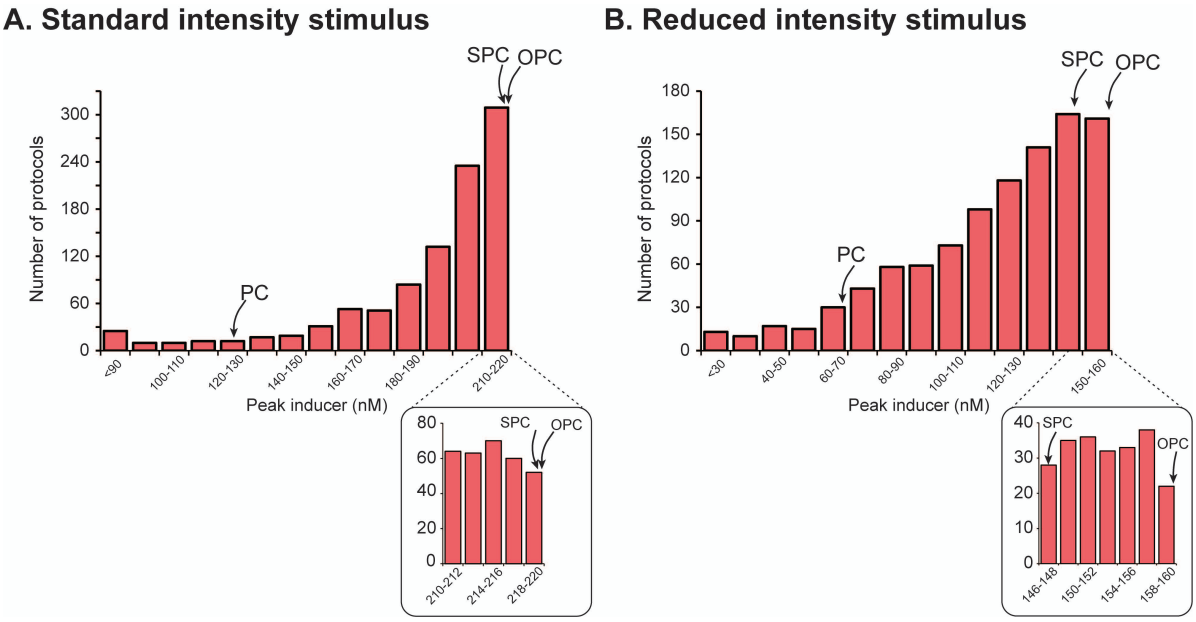

515

516 **Figure 3**. **Histogram of peak levels of *inducer* from 1,000 protocols. A**, Standard intensity
517 stimulus (*Stim* = 300 μM). The range of peak levels of *inducer* (0 – 220 nM) was subdivided into

518 14 bins, and the number of simulations that produced a peak concentration of *inducer* in each
519 subdivision was plotted. The arrows indicate which bins contained the peak concentrations
520 produced by the partial conditioning, spaced partial conditioning (SPC), and optimal partial
521 conditioning (OPC) protocols. **B,** Reduced intensity stimulus (*Stim* = 200 μM). The range of peak
522 levels of *inducer* (0 – 160 nM) was subdivided into 14 bins, and the number of simulations that
523 produced a peak concentration of *inducer* in each subdivision was plotted. Insets below the main
524 plots illustrate in detail the difference in peak *inducer* for SPC *vs*. OPC, which is negligible in **A**.

525

526 To test this prediction, we empirically compared the OPC and SPC protocols using a
527 reduced shock intensity (0.5 mA instead of the 0.7 mA used in Fig. 2) (**Fig. 4B**). Rats
528 were assigned to OPC or SPC groups by matching their baseline freezing and locomotor
529 activity during the familiarization session. No significant difference was found between
530 their baseline freezing level (SPC: 3.72%, OPC: 5.21%, Unpaired Student's t-test, t_{16} =
531 0.988, P = 0.337), average speed (SPC: 0.016 m/s, OPC: 0.015 m/s, one-way ANOVA,
532 $F_{(2, 37)}$ = 0.062, P = 0.939), and maximum speed (FC: 0.439 m/s, PC: 0.424 m/s, OPC:
533 0.446 m/s, one-way ANOVA, $F_{(2, 37)}$ = 0.044, P = 0.956). During the fear acquisition, the
534 SPC group received 4 CS-US pairings with ITIs of 11 min and 10 s, whereas the OPC
535 group was exposed to the same protocol as in Fig. 2 (*i.e.*, 4 CS-US pairings with ITIs of
536 8, 8, and 16 min) (**Fig. 4C**). We found that the difference in the ITIs between the OPC
537 and SPC groups was sufficient to result in distinct levels of fear memory acquisition. Rats
538 exposed to OPC showed higher CS freezing levels during the third CS-US pairing of the
539 fear acquisition session (**Fig. 4D Day 1;** Two-way RM ANOVA followed by Tukey's
540 planned comparison. $F_{(4, 64)}$ = 1.550, P = 0.339; OPC vs. SPC: p = 0.019). In addition,

541 fear memory retrieval was increased when rats in the OPC group were returned to context
542 A for an extinction training session on Day 3, as indicated by higher freezing during the
543 first two CS presentations, compared to the SPC group (**Fig. 4D Inset;** Welch's t-test.
544 $t_{12.43} = 2.227$, $p = 0.045$). Both OPC and SPC groups exhibited the same levels of freezing
545 by the end of the extinction training session (**Fig. 4D Day 3;** Two-way RM ANOVA
546 followed by Tukey's post hoc test. $F_{(11, 176)} = 2.997$, $P = 0.001$; Tone 12, OPC vs. SPC:
547 $p > 0.999$), as well as during the extinction retrieval tests performed in context A (**Fig. 4D**
548 **Day 4;** Two-way RM ANOVA. $F_{(2, 37)} = 0.097$, $P = 0.907$) or context B (**Fig. 4D Day 5;**
549 Two-way RM ANOVA. $F_{(2, 37)} = 2.984$, $P = 0.629$). However, fear memory spontaneously
550 recovered when rats in the OPC group were retested in context A approximately 3 weeks
551 later, as indicated by higher freezing during the first CS presentation compared to SPC-
552 trained rats (**Fig. 4D Day 29;** Two-way RM ANOVA followed by Tukey's planned
553 comparison. $F_{(2, 32)} = 1.809$, $P = 0.180$; OPC vs. SPC: $p = 0.030$). In summary, these data
554 suggest that the enhancement in fear memory acquisition observed with our
555 computationally designed OPC protocol cannot simply be attributed to a trial-spacing
556 effect or differences in the delay to remove the animals from the chamber, but it is rather
557 associated with the maximized overlap between PKA and ERK signaling.

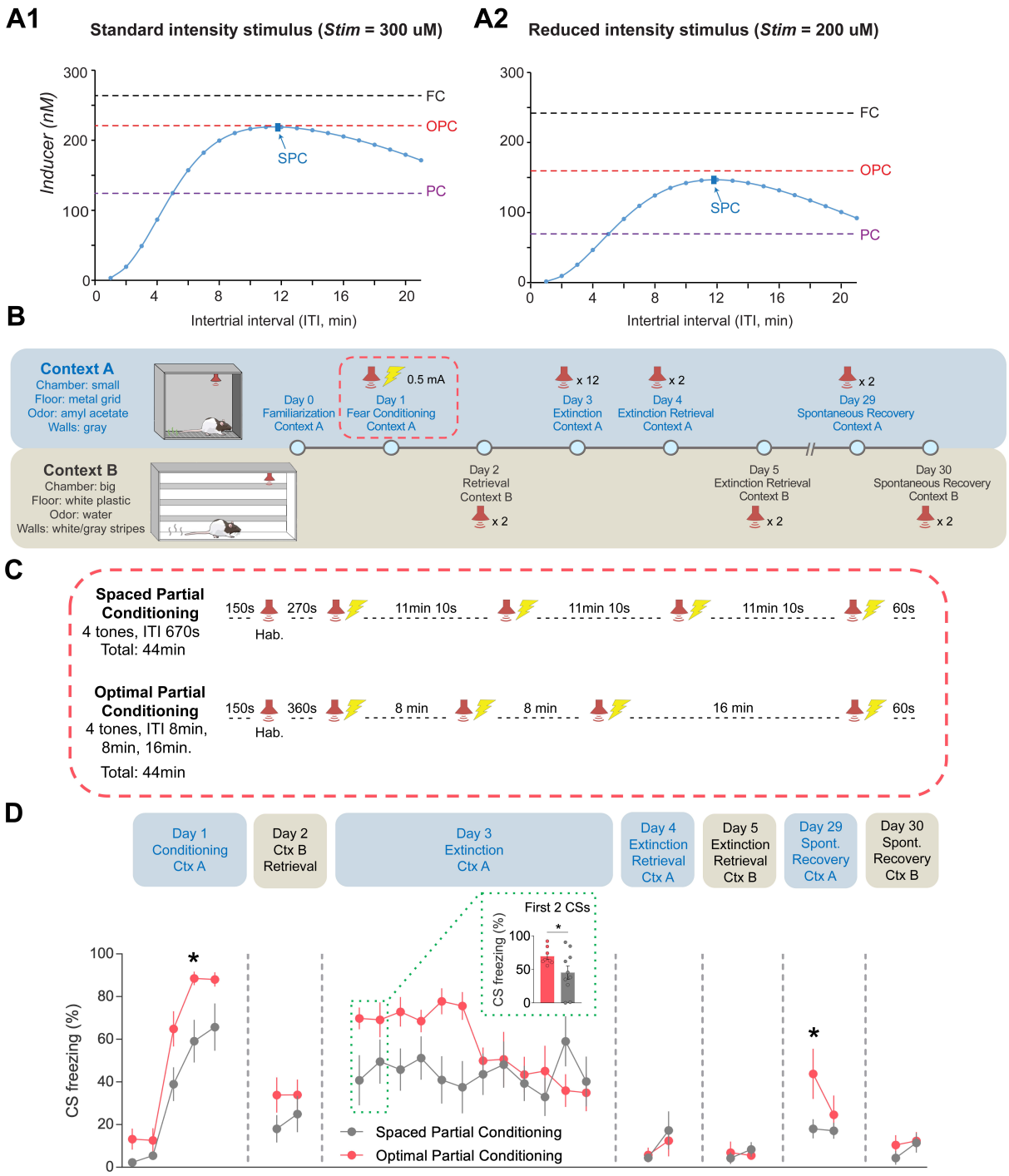

Figure 4. **Optimal partial conditioning protocol induced stronger fear memory than spaced partial conditioning protocol in rats**. **A**, *Inducer* peak levels from the FC, PC, and OPC protocols, compared to peak levels from partial conditioning protocols of 4 trials with regular ITIs

562 varying from 1 to 21 min, using standard intensity stimulus (**A1**) or reduced intensity stimulus (**A2**).
563 The peak *inducer* values of FC, PC, and OPC are labeled by dashed lines (black: FC; red: OPC;
564 purple: PC). The blue curve gives peak *inducer* values for the protocols with regular ITIs, and the
565 curve peaks at the dark blue dot and arrow, representing the SPC protocol with equal ITIs of 11
566 min and 10 s. **B,** Schematics of the fear conditioning procedures. Top: tests that were conducted
567 in Context A. Bottom: tests that were conducted in Context B. **C,** Schematics of the fear
568 conditioning protocols for OPC (n = 8), and SPC, (n = 10, ITI = 670 s) groups. Following a
569 habituation (Hab.) tone, rats received 4 trials of a CS (3 kHz tone, 30 s) that co-terminated with a
570 US (footshock, 0.5 mA, 0.5 s). **D,** Freezing levels during CS presentations of each group across
571 the experiment; Two-way repeated-measure ANOVA for each day followed by Tukey's pairwise
572 post hoc test, * $p<0.05$. Inset: the average freezing level during the first two CS presentations;
573 Welch's t-test, * $p<0.05$.
574

575 **The optimal partial conditioning protocol induces greater levels of phosphorylated**
576 **CREB in DG than a spaced partial conditioning protocol**

577 The computational model predicts that the increased overlap of PKA and ERK activation
578 in OPC protocol leads to greater LTP induction in rat hippocampus. One of the
579 mechanisms that may enhance LTP is increased convergence of the PKA and ERK
580 pathways to induce phosphorylation of CREB (Impey et al., 1998), a transcription factor
581 required for synaptic plasticity and LTP (Liu et al., 2011; Bourtchuladze et al., 1994; See
582 review by Kida, 2012). We therefore used immunohistochemistry to quantify the levels of
583 pCREB in rat dorsal hippocampus following fear conditioning in OPC versus SPC groups.
584 We repeated the same experimental design used in **Fig 4,** as the observed augmentation
585 in fear acquisition was predicted to correlate with differences in pCREB levels between

586 the two groups following fear conditioning (**Fig. 5A**). Rats were assigned to OPC or SPC
587 groups by matching their baseline freezing and locomotor activity during the
588 familiarization session. No significant difference was found between their baseline
589 freezing level (SPC: 5.90%, OPC: 8.53%, Unpaired Student's t-test, $t_5 = 0.677$, $p = 0.528$),
590 average speed (SPC: 0.014 m/s, OPC: 0.015 m/s, Unpaired Student's t-test, $t_5 = 0.239$ p
591 = 0.820), and maximum speed (SPC: 0.272 m/s, OPC: 0.367 m/s, Unpaired Student's t-
592 test, $t_5 = 1.697$, $p = 0.150$). During the fear acquisition session, rats exposed to the OPC
593 or SPC protocols showed similar levels of freezing during the CS presentations (**Fig. 5B**,
594 Two-way RM ANOVA. $F_{(4, 20)} = 0.848$, $P = 0.5112$. Inset, Unpaired Student's t-test, t_5 =
595 2.405, p = 0.061), most likely due to the reduced sample sizes. However, OPC rats
596 reached significantly higher levels of CS freezing during the end of the conditioning
597 session (Unpaired Student's t-test, $t_5 = 2.769$, $p = 0.039$). Approximately 15 min after the
598 end of fear acquisition session, rats were perfused and their brains were collected for
599 subsequent analyses. Immunohistochemistry revealed high levels of pCREB expression
600 across different hippocampal subfields in both OPC and SPC groups, with the highest
601 expression level being observed in the DG (**Fig. 5C**; Two-way ANOVA followed by
602 Tukey's post-hoc test. $F_{(3, 20)} = 4.533$, $P = 0.014$; CA1 vs. DG: $p < 0.001$; CA2 vs. DG: p
603 < 0.001; CA3 vs. DG: $p < 0.001$). Interestingly, rats exposed to the OPC protocol exhibited
604 increased pCREB expression in the DG when compared to the SPC group (**Fig. 5C-D;**
605 Two-way ANOVA followed by Bonferroni's post-hoc test. $F_{(3, 20)} = 4.533$, $P = 0.014$; OPC
606 vs. SPC: $p = 0.004$). Given that increased pCREB levels in the DG has been associated
607 with the induction efficiency of LTP in rodents (Davis et al., 2000), our immunostaining
608 results support the prediction that the augmentation in fear memory acquisition observed

609 with the OPC protocol is mediated by higher levels of LTP induction in the rat

610 hippocampus.

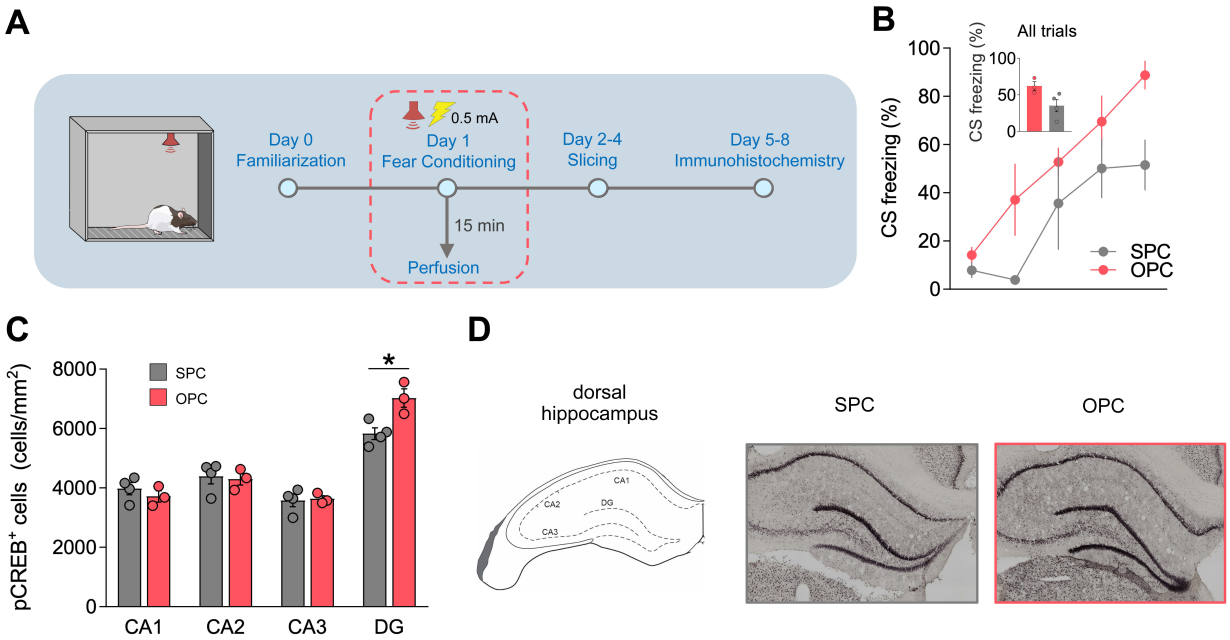

611

612 **Figure 5**. **Immunohistochemistry quantification of pCREB in hippocampus of rats exposed**

613 **to optimal versus spaced partial conditioning protocols**. **A,** Schematic of the

614 immunohistochemistry procedure. **B,** Freezing levels during CS presentation for OPC (n = 3) and

615 SPC (n = 4) groups during fear conditioning; Two-way RM ANOVA followed by Bonferroni

616 correction. Inset, averaged freezing level for the 4 CS presentations; Student's t-test. **C,** Average

617 pCREB density across hippocampal subfields for OPC (n = 3) and SPC (n = 4) groups; Two-way

618 ANOVA followed by Tukey's Bonferroni correction. *$p < 0.05$. **D**, Representative images of pCREB

619 immunostaining in distinct subfields of the dorsal hippocampus (left) in the SPC group (middle)

620 and OPC group (right).

621

622 **The optimal partial protocol also enhanced fear extinction**

623 Extinction is a new learning that temporarily inhibits the initial associative memory (de

624 Oliveira Alvares and Do-Monte, 2021; Quirk and Mueller, 2008). Because previous

625 studies suggest that the molecular mechanisms underlying fear extinction learning are
626 similar to those underlying fear acquisition (Berman and Dudai, 2001; Flood et al., 1977;
627 Radulovic and Tronson, 2010; Santini et al., 2001; Szapiro et al., 2003; Tronson et al.,
628 2008), we hypothesized that the computationally designed protocol would also enhance
629 the acquisition of extinction, suppressing the original fear memory (**Fig. 6A-B1**). We
630 therefore used the OPC protocol with 4 trials and irregular ITIs of 8, 8, and 16 min as an
631 Optimal Partial Extinction (OPE) protocol (**Fig. 6B4**). We compared the OPE protocol with
632 a Full Extinction (FE, **Fig. 6B2**) protocol using 12 trials and ITIs of 150 s, and a Partial
633 Extinction (PE, **Fig. 6B3**) protocol using 4 trials and the same ITIs of 150 s, which
634 resemble previous protocols used for full and partial fear extinction in rats (Santini et al.,
635 2004; Holmes and Quirk, 2010; Do-Monte et al., 2015). Similar to the simulation results
636 for the conditioning protocols, the OPE protocol triggered higher peak *inducer* than the
637 PE protocol with equal ITIs of 150 s, and was comparable to the FE protocol (**Fig. 6B**).
638 We thus predicted the OPE protocol would result in stronger extinction of fear memory
639 than the standard PE protocol.
640

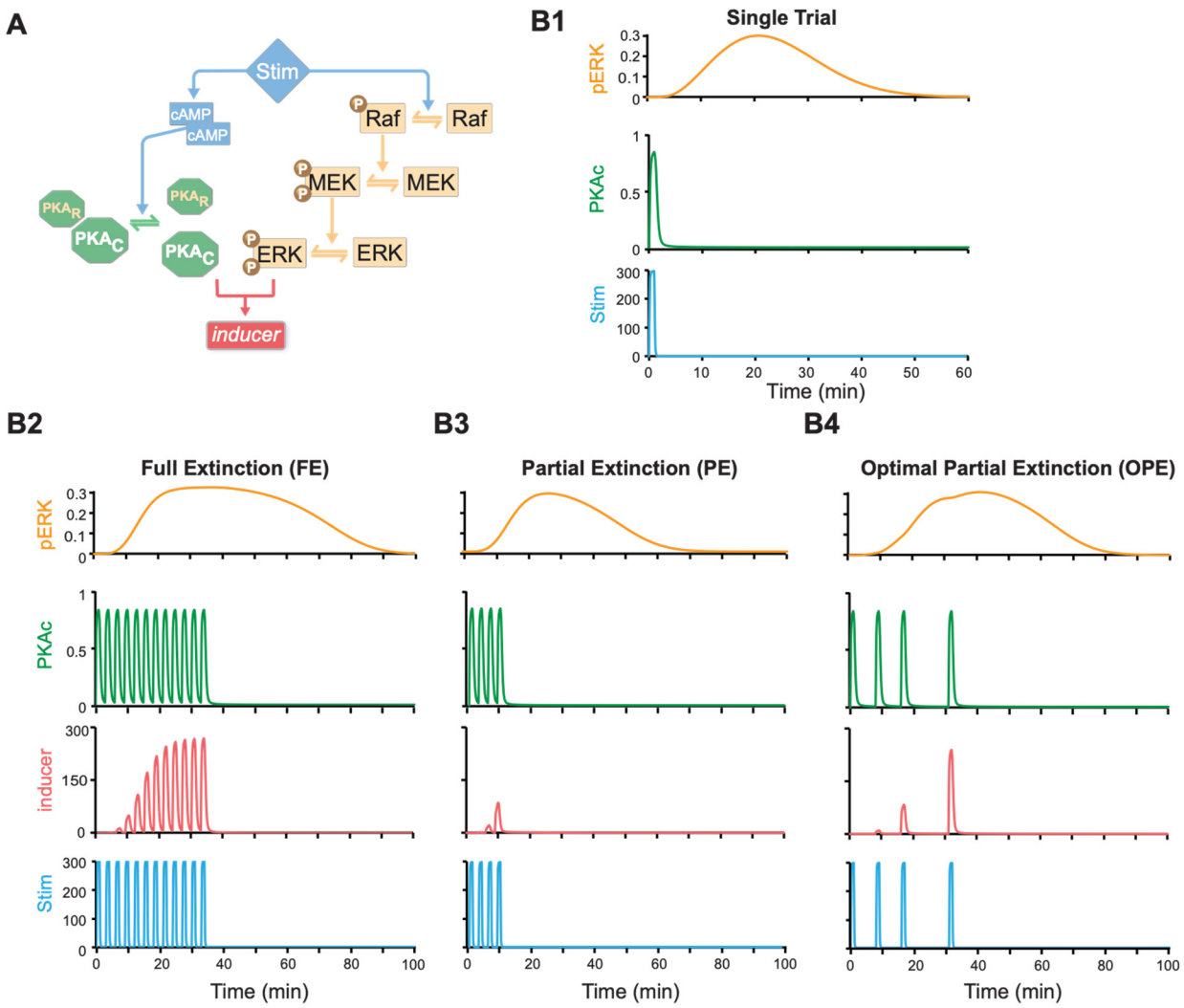

Figure 6. Prediction of enhanced protocol for fear extinction. A, Schematic of the model. **B1**, Simulated time courses of activated ERK (pERK, μM) and activated PKA (PKAc, μM) in response to one trial of *Stim* (μM). **B2**, Simulated time courses of pERK, PKAc, and *inducer* (nM) in response to 12-trial protocol with regular intervals of 2.5 min (full extinction, FE). **B3**, Simulated time courses of pERK, PKAc, and *inducer* in response to 4-trial protocol with regular intervals of 2.5 min (partial extinction, PE). **B4**, Simulated time courses of pERK, PKAc, and *inducer* in response to 4-trial protocol with computationally designed intervals (optimal partial extinction, OPE).

650 To test this prediction, we designed an experiment comparing the efficacy of different
651 extinction protocols (**Fig. 7A**). We used conditioned suppression of reward-seeking
652 behavior as an additional measure of fear memory because lever-press suppression is
653 more sensitive than freezing during fear extinction paradigms (Mast et al., 1982; Sotres-
654 Bayon et al., 2012). In addition, lever presses help to maintain a constant level of activity
655 so that freezing can be more reliably measured along the session (Quirk et al., 2000).
656 Since lever presses for reward are trained in a specific context, and extinction memory is
657 context-dependent (Podlesnik et al., 2017; Goode and Maren, 2014), we used only one
658 context in this experiment so that lever press suppression can be consistently assessed
659 across sessions and the extinction memory can be retrieved after the extinction learning.
660 Rats were initially trained to press a lever to receive sucrose pellets in a variable interval
661 schedule of 60 s. After 7 days of training, rats reached the same levels of lever pressing
662 (~10 presses/min) and locomotor activity. On Day 8, they underwent a fear conditioning
663 session which included five nonreinforced habituation tones (3 kHZ, 75 dB, 30 s duration)
664 followed by seven CS-US pairings (ITIs of 150 s, 37 min duration). In simulations, the
665 OPE group showed peak levels of *inducer* comparable to the FE group and higher than
666 the PE group when strong stimuli were used (**Fig. 6**). We therefore increased the
667 footshock intensity from 0.7 mA to 1.0 mA, which resulted in stronger fear acquisition and
668 consequently higher freezing levels during the extinction session. This stimulus intensity
669 also helped to avoid a “floor effect” in the following tests. On Day 9, rats were assigned
670 to three experimental groups by matching their freezing and lever presses during the fear
671 conditioning session: Full Extinction (FE), Partial Extinction (PE), and Optimal Partial
672 Extinction (OPE) (One-way ANOVA. $F_{(14, 231)} = 0.404$, $P = 0.973$). No significant difference

673 was found among their freezing level (FE: 3.20%, PE: 4.43%, OPE: 3.07%, Kruskal-
674 Wallis's test $H(2)$ = 0.188, P = 0.910), average speed (FE: 0.036 m/s, PE: 0.036 m/s,
675 OPE: 0.037 m/s, one-way ANOVA, $F_{(2, 33)}$ = 0.042, P = 0.958), and lever presses (FE:
676 11.13 presses/min, PE: 9.64 presses/min, OPE: 9.603 presses/min, one-way ANOVA, $F_{(2,}$
677 $_{33)}$ = 0.480, P = 0.622). On Day 10, rats were returned to the same chamber for a fear
678 extinction session (39 min duration). The FE group received twelve CSs with ITIs of 150
679 s; the PE group received four CSs with ITIs of 150 s and remained in the chamber until
680 the end of the session; and the OPE group received four CSs with ITIs of 8, 8, and 16
681 min (**Fig. 7B**). Our results revealed that at the end of the CS presentations, freezing levels
682 reduced from ~50% to ~20% in the FE groups, whereas the PE and OPE groups
683 maintained the same levels of freezing throughout the four CSs (**Fig. 7C**, Day 8). Similarly,
684 the FE group showed a significant increase in lever presses (from 0.1 to 1.5 press/min)
685 during the CS presentations from the beginning to the end of the session, whereas CS
686 lever presses remained unaltered in the PE and OPE groups (paired Student's t-test; FE,
687 first 4 CS lever presses: 0.08 presses/min, last 4 CS lever presses: 1.5 presses/min, t_{11}
688 = 2.837, p = 0.016; PE, first 4 CS lever presses: 0 presses/min, last 4 CS lever presses:
689 0.18 presses/min, t_{10} = 1.000, p = 0.341; OPE, first 4 CS lever presses: 0.46 presses/min,
690 last 4 CS lever presses: 1.23 presses/min, t_{12} = 1.237, p = 0.239). However, the OPE
691 group showed a significant increase in lever presses during the 30-s periods that
692 preceded the CS presentations (pre-CS) when comparing the first two pre-CS periods to
693 the last pre-CS period of the extinction training session (**Fig. 7D&E**; Paired Student's t-
694 test; FE: t_{11} = 0.994, p = 0.341; PE: t_{10} = 1.111, p = 0.293; OPE: t_{12} = 3.773, p = 0.003),
695 suggesting enhanced within-session extinction of contextual fear memory (Morgan and

696 LeDoux, 1995). On Days 10 and 35, rats were returned to the same chamber and
697 received two CSs with an ITI of 150 s to test the strength of fear extinction memory during
698 extinction retrieval and spontaneous recovery tests, respectively. No significant difference
699 in CS freezing or CS lever presses were observed among the three groups during these
700 tests (**Fig. 7C, Day 10&35;** Two-way RM ANOVA. Day 10: Freezing, $F_{(2, 33)} = 0.207$, $P =$
701 0.814; Lever Presses, $F_{(2, 33)} = 0.069$, $P = 0.933$; Day 35: Freezing, $F_{(2, 33)} = 0.535$, $P =$
702 0.591; Lever Presses, $F_{(2, 33)} = 1.085$, $P = 0.350$). However, the OPE group showed
703 increased pre-CS lever pressing rate either in the first pre-CS period (**Fig. 7D;** Two-way
704 RM ANOVA followed by Tukey's planned comparison. $F_{(2, 33)} = 2.897$, $P = 0.069$; Tone 1,
705 a, FE vs. PE, p = 0.791; b, FE vs. OPE, p = 0.025; c, OPE vs. PE, p = 0.005) or when
706 averaging the two pre-CS periods during the spontaneous recovery test (**Fig. 7F**; Kruskal-
707 Wallis's test followed by Dunn's post hoc test. $H(2) = 6.414$, $P = 0.041$; a: FE vs. OPE, p
708 = 0.531; b: FE vs. PE, p = 0.709; c: OPE vs. PE, p = 0.035), when compared to the FE
709 and PE groups on day 35. These results suggest that, although the tone-associated
710 memory was similar among the groups, our computationally designed OPE protocol was
711 able to enhance the extinction of contextual fear memory, as indicated by enhanced
712 within-session extinction of conditioned suppression and by reduced conditioned
713 suppression approximately 3 weeks after the extinction training session.
714

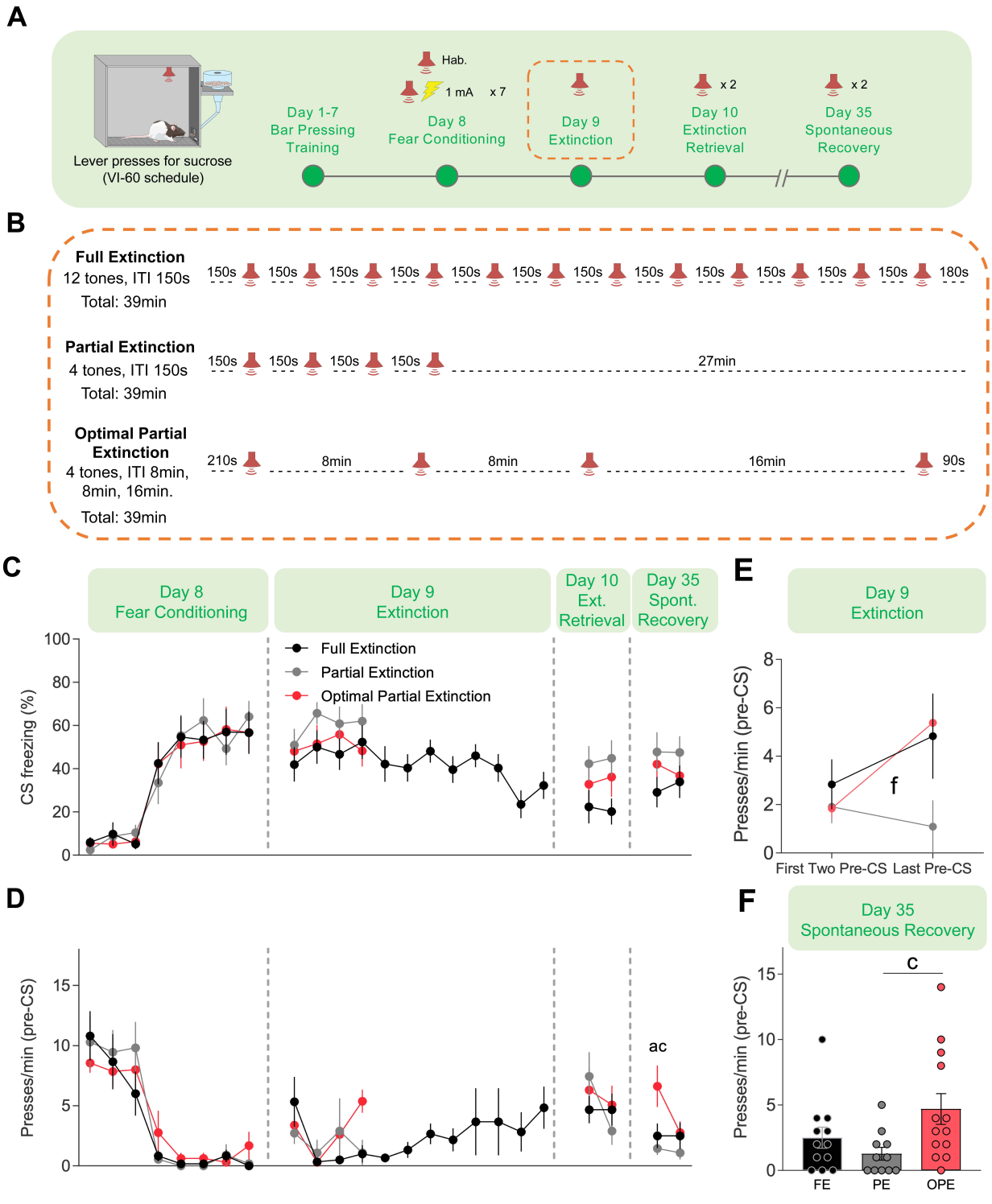

Figure 7. Computationally designed protocol enhanced fear extinction in rats. **A.** Schematic of the enhanced fear extinction experimental procedures. Rats were trained to constantly press a lever to retrieve sucrose pellets in a variable interval 60 (VI60) schedule, where the average interval between each sucrose delivery is 60 s. **B,** Schematics of the fear extinction protocols for

720 FE (n = 12), PE (n = 11), and OPE (n = 13) groups, during which rats received multiple trials of a
721 CS (3 kHz tone, 30 s). **C,** Freezing levels during CS presentations of each group across the
722 experiment. No significant difference between groups was found by Two-way RM ANOVA. **D,**
723 Lever press rates during the 30 s of each CS presentation (pre-CS period) of each group across
724 the experiment. Two-way repeated-measure ANOVA for each day followed by Tukey's pairwise
725 post hoc test. Letters a and c indicate pairwise tests with $p < 0.05$: a, FE vs. OPE ; c, OPE vs. PE.
726 **E,** OPE group shows significant increase of pre-CS lever presses comparing the last CS
727 presentation to the average lever press rate of the first two CS presentations. Paired Student's t-
728 test. Letter f indicates test with $p < 0.05$: OPC, Last 4 CS vs. First 4 CS. **F,** OPE group shows
729 higher lever presses during pre-CS period compared to PE group in spontaneous recovery test.
730 One-way ANOVA followed by Tukey's post hoc test. Letter c indicates pairwise comparison with
731 * $p<0.05$: OPE vs. PE.
732

733 **DISCUSSION**

734 Studies on nonassociative learning in invertebrates have provided significant insights
735 about the molecular mechanisms of learning and memory due to their simplicity and
736 tractability (Byrne and Hawkins, 2015; Kandel, 2001; Carew and Sahley, 1986). Long-
737 term nonassociative learning in different regions of the nervous system or across different
738 species shares many intracellular molecular cascades including cAMP-PKA and Raf-
739 MEK-ERK signaling (Bartsch et al., 1995; Martin et al., 1997). These two pathways are
740 also required for associative learning in invertebrates and mammals (Hawkins and Byrne,
741 2015; Schafe and LeDoux, 2000; Adams and Sweatt, 2002). The conservation of these
742 mechanisms makes these molecular cascades potential candidates for a universal
743 intervention to enhance learning and memory. We have previously demonstrated that a

744 computationally designed protocol that maximizes the interaction between PKA and ERK
745 pathways enhances LTF and nonassociative learning in *Aplysia* (Zhang et al., 2011).
746 Here, we extended the feasibility of this computational approach to associative learning
747 in mammals by adapting the simplified mathematical model used in *Aplysia* to simulate
748 the dynamics of PKA and ERK in rat hippocampus based on empirical data available in
749 the literature (Wang et al., 2014; Roberson and Sweatt, 1996; Vázquez et al., 2000). After
750 simulating ~1000 different training protocols of auditory fear conditioning, we identified an
751 optimal protocol with irregular ITIs which resulted in stronger fear acquisition and
752 extinction-resistant memory formation in rats, when compared to either massed or spaced
753 training protocols with equal ITIs. Immunohistochemical staining demonstrated that the
754 augmented fear memory induced by the OPC protocol was associated with increased
755 expression levels of pCREB in the DG subfield of the dorsal hippocampus. Using a
756 separate fear extinction paradigm, we also showed that an optimal training protocol was
757 sufficient to induce enhanced extinction of contextual fear memory in rats, when
758 compared to standard or partial extinction protocols with equal ITIs. Our results
759 demonstrate the power of a simplified model of intracellular signaling cascades in guiding
760 associative learning across species, attesting the essential role of the interaction between
761 PKA and ERK pathways in both nonassociative and associative learning. In addition, our
762 findings highlight the potential clinical relevance of using computational modeling to
763 enhance associative learning in patients with memory deficits, as well as to enhance
764 extinction-based exposure therapies in patients with anxiety disorders.
765

766 Pioneering studies have demonstrated that training protocols using spaced ITIs result in
767 stronger memory acquisition than those using standard massed ITIs, a well-established
768 phenomenon described as the "spacing effect" (see review by Smolen et al., 2016). Data
769 demonstrating this effect in animals and humans illustrate the relationship between the
770 duration of the ITIs and the strength of memory formation as an inverted-U-shape curve
771 (Verkoeijen et al., 2005; Barela, 1999), consistent with our simulated results (**Fig. 1**).
772 Previous findings have attributed this spacing effect to the different efficacy of massed vs.
773 spaced protocols in inducing LTP/LTF through plasticity-related signaling. For instance,
774 spaced training protocols in rodents lead to increased activation of ERK (Ajay and Bhalla,
775 2007), followed by CREB phosphorylation and the expression of downstream genes,
776 which have not been reported following massed training protocols in the same species
777 (Genoux et al., 2002). A computational model based on slice electrophysiology from rat
778 hippocampal data has found that the peak of ERK activation aligns with the optimal ITI
779 for LTP induction (Ajay and Bhalla, 2004). Although that study provided a possible
780 mechanism for the trial-spacing effect and a potential approach to identify more effective
781 protocols for associative learning, it relied on fixed ITIs that are not necessarily the optimal
782 intervals to induce synaptic plasticity and LTM. In fact, our simulations showed that an
783 optimal protocol with irregular ITIs was superior to most spaced protocols with the same
784 number of trials and equal ITIs. In the fear conditioning experiment, the optimal protocol
785 induced stronger and persistent fear memory in rats, when compared to a spaced protocol
786 predicted to be the most efficient among protocols with equal ITIs. These results suggest
787 that the trial-spacing effect in mammals can be at least partially explained by enhanced
788 overlap between PKA and ERK pathways, which are critical for CREB activation (Impey

789 et al., 1998). More importantly, our findings demonstrate that protocols that include
790 irregular ITIs can be a better approach to enhance learning than previous protocols using
791 equal ITIs.
792
793 The enhanced performance of our optimal protocol (OPC) compared to a spaced protocol
794 (SPC) during fear conditioning appears constrained by the intensity of stimuli. The model
795 predicts higher performance for OPC when weak stimuli are used, but comparable
796 performance when strong stimuli are used (**Fig. 4A**). Drawing a line to distinguish weak
797 and strong footshock intensities is not straightforward because the relationship between
798 fear memory and footshock intensity is neither monotonic nor linear (Davis and Astrachan,
799 1978). Nevertheless, we observed clear differences in the efficacy of the optimal fear
800 conditioning protocol when using footshocks of different intensities. When we compared
801 the optimal partial conditioning protocol to a massed partial conditioning protocol using a
802 standard footshock intensity (0.7 mA, **Fig. 2**) commonly used in previous studies (Abel et
803 al., 1997), we found only small differences in the conditioned responses (CS freezing)
804 between the two protocols. However, when we used a lower footshock intensity (0.5 mA,
805 **Fig. 4**) to compare the optimal partial conditioning protocol to a spaced partial
806 conditioning protocol, we found a significant increase in CS freezing in the OPC group
807 during fear acquisition, retrieval, and spontaneous recovery tests. Considering the
808 robustness of the spacing effect, it is possible that differences between the OPC and the
809 massed PC groups at the higher footshock intensity were masked by a “ceiling effect”.
810 These data suggest that our approach could be more beneficial for learning protocols
811 relying on relatively weak stimuli. Additional studies need to be conducted to understand

812 the mechanism by which the intensity of stimuli determines the enhanced performance of
813 protocols with irregular ITIs compared to protocols with fixed ITIs.
814
815 The association between the CS and US is primarily mediated by the lateral amygdala
816 where LTP induces enhanced CS responses (see review by Maren, 2005; Johansen et
817 al., 2011). Nevertheless, another important and distinguishable component of fear
818 memory formation is the context in which the association has occurred. In the fear
819 conditioning experiment, enhanced CS freezing was only observed in the same context
820 where fear conditioning took place, suggesting that the memory facilitation effect induced
821 by our optimal protocol is context dependent. Similarly, in the fear extinction experiment,
822 enhancement by the optimal protocol was only observed during the pre-CS lever pressing,
823 a more sensitive index of contextual fear memory during extinction and spontaneous
824 recovery (Morgan and LeDoux, 1995; Padilla-Coreano et al., 2012; Woods and Bouton,
825 2008; Sotres-Bayon et al., 2012; Mast et al., 1982). These results are consistent with
826 current empirical data from rat hippocampus, on which our model is based. The
827 hippocampus plays major roles in context encoding during fear conditioning, fear
828 extinction, and the time-dependent reappearance of fear following extinction training (*i.e.*,
829 spontaneous recovery) (see reviews by Maren et al., 2013; Bouton et al., 2021).
830 Accordingly, our immunohistochemical results showed greater pCREB expression
831 specifically in the DG of the dorsal hippocampus, a region implicated in the acquisition
832 and extinction of contextual fear memory (Kheirbek et al., 2013; Bernier et al., 2017).
833 Increasing CREB expression in DG neurons using a viral approach has been
834 demonstrated to improve contextual fear acquisition (Restivo et al., 2009), whereas

835 chemogenetically or optogenetically inactivating DG neurons that overexpress CREB
836 disrupts contextual fear retrieval (Park et al., 2016).
837
838 Another hippocampal subregion implicated in contextual fear is the CA1 (Hunsaker and
839 Kesner, 2008). Although the OPC and SPC groups displayed similar levels of pCREB
840 expression in CA1, the single post-training time point we used do not suffice to rule out
841 the possibility of distinct pCREB dynamics in CA1 compared to DG. Indeed, prior reports
842 have shown that CA1 pCREB expression peaks at 30 min and disappears at 90 min
843 following fear conditioning (Sindreu et al., 2007; Chaaya et al., 2019), a timeframe that
844 differs from the 15 min post-training interval we used to detect group differences in DG
845 pCREB expression. Further experiments comparing distinct post-training intervals may
846 better reveal the dynamics of pCREB expression in different hippocampal subregions, as
847 well as in non-hippocampal areas involved in fear acquisition such as the lateral amygdala.
848 The observation that the dynamics of ERK pathways differ across brain regions involved
849 in fear memory, with peaks occurring at 20 min after stimulation in the hippocampus
850 versus 60 min after fear conditioning in the lateral amygdala (Schafe et al., 2000; Di
851 Benedetto et al., 2009; Wang et al., 2014), suggests that the model may be able to predict
852 optimal protocols targeting specific components of fear memory based on the dynamics
853 of intracellular signaling cascades in distinct brain regions. Future studies will test this
854 possibility by modeling the molecular cascades in the lateral amygdala and the medial
855 prefrontal cortex to preferentially target the acquisition and extinction of CS-associated
856 memories, respectively.
857

858 It is worth noting that the model is rather simplified. We did not consider many other
859 important molecular cascades critical for LTP and memory formation. For example,
860 calcium/calmodulin-dependent protein kinase II (CaMKII) and protein kinase C (PKC) are
861 also required for LTP induction (Smolen et al., 2020; Malenka et al., 1989; Wang et al.,
862 2016). In addition, we built the model with empirical data of PKA and ERK dynamics from
863 the literature, which are based on *ex vivo* analyses and have limited temporal resolution.
864 However, despite these limitations, the simplified model using essential biochemical
865 cascades for learning and memory was sufficient to enhance activation of the LTP-related
866 transcription factor CREB in the DG and facilitate associative learning in three different
867 experiments in mammals. A more complex model that incorporates a wider range of
868 intracellular and extracellular processes based on *in vivo* real-time data would likely
869 strengthen the predictive ability of simulations. Further experiments should also
870 investigate whether the memory enhancing effects of the optimal protocol vary across
871 subjects of different sexes and ages, as well as its efficacy in animal models of cognitive
872 impairment. Together, our results suggest the possibility of using similar model-driven,
873 non-invasive behavioral approaches in preclinical and clinical studies aimed at enhancing
874 learning or restoring memory deficits in humans.
875
876 **Author Contributions:** X.O.Z, D.S.E., and C.E.C performed and analyzed the behavioral
877 experiments. X.O.Z and C.E.C performed and analyzed the immunohistochemistry
878 experiments. Y.Z. implemented the computational model and ran all simulations. P.S.
879 helped design and implement the computational model. F.H.D-M and J.H.B supervised
880 and contributed to all aspects of this study. All the authors participated in the design of

881 the experiments. X.O.Z. and F.H.D-M interpreted the data and prepared the manuscript

882 with comments from all the co-authors.

883

884 **REFERENCES**

885 Abel T, Nguyen PV, Barad M, Deuel TA, Kandel ER, Bourtchouladze R (1997) Genetic
886 demonstration of a role for pka in the late phase of ltp and in hippocampus-based
887 long-term memory. Cell 88:615-626.

888 Adams JP, Sweatt JD (2002) Molecular psychology: Roles for the erk map kinase
889 cascade in memory. Annu Rev Pharmacol Toxicol 42:135-163.

890 Ajay SM, Bhalla US (2004) A role for erkii in synaptic pattern selectivity on the time-
891 scale of minutes. Eur J Neurosci 20:2671-2680.

892 Ajay SM, Bhalla US (2007) A propagating erkii switch forms zones of elevated dendritic
893 activation correlated with plasticity. HFSP J 1:49-66.

894 Alberini CM (2009) Transcription factors in long-term memory and synaptic plasticity.
895 Physiol Rev 89:121-145.

896 Anderson MJ, Jablonski SA, Klimas DB (2008) Spaced initial stimulus familiarization
897 enhances novelty preference in long-evans rats. Behav Processes 78:481-486.

898 Bankhead P, Loughrey MB, Fernandez JA, Dombrowski Y, McArt DG, Dunne PD,
899 McQuaid S, Gray RT, Murray LJ, Coleman HG, James JA, Salto-Tellez M,
900 Hamilton PW (2017) Qupath: Open source software for digital pathology image
901 analysis. Scientific reports 7:16878.

902 Barela PB (1999) Theoretical mechanisms underlying the trial-spacing effect in
903 pavlovian fear conditioning. J Exp Psychol Anim Behav Process 25:177.

904 Bartsch D, Ghirardi M, Skehel PA, Karl KA, Herder SP, Chen M, Bailey CH, Kandel ER
905 (1995) Aplysia creb2 represses long-term facilitation: Relief of repression

906 converts transient facilitation into long-term functional and structural change. Cell
907 83:979-992.
908 Berman DE, Dudai Y (2001) Memory extinction, learning anew, and learning the new:
909 Dissociations in the molecular machinery of learning in cortex. Science
910 291:2417-2419.
911 Bernier BE, Lacagnina AF, Ayoub A, Shue F, Zemelman BV, Krasne FB, Drew MR
912 (2017) Dentate gyrus contributes to retrieval as well as encoding: Evidence from
913 context fear conditioning, recall, and extinction. J Neurosci 37:6359-6371.
914 Bourtchuladze R, Frenguelli B, Blendy J, Cioffi D, Schutz G, Silva AJ (1994) Deficient
915 long-term memory in mice with a targeted mutation of the camp-responsive
916 element-binding protein. Cell 79:59-68.
917 Bouton ME, Maren S, McNally GP (2021) Behavioral and neurobiological mechanisms
918 of pavlovian and instrumental extinction learning. Physiol Rev 101:611-681.
919 Brown MT, Tan KR, O'Connor EC, Nikonenko I, Muller D, Luscher C (2012) Ventral
920 tegmental area gaba projections pause accumbal cholinergic interneurons to
921 enhance associative learning. Nature 492:452-456.
922 Byrne JH, Hawkins RD (2015) Nonassociative learning in invertebrates. Cold Spring
923 Harb Perspect Biol 7.
924 Cain CK, Blouin AM, Barad M (2003) Temporally massed cs presentations generate
925 more fear extinction than spaced presentations. J Exp Psychol Anim Behav
926 Process 29:323-333.
927 Carew TJ, Sahley CL (1986) Invertebrate learning and memory: From behavior to
928 molecules. Annu Rev Neurosci 9:435-487.

929 Cepeda NJ, Pashler H, Vul E, Wixted JT, Rohrer D (2006) Distributed practice in verbal
930 recall tasks: A review and quantitative synthesis. Psychol Bull 132:354-380.
931 Chaaya N, Jacques A, Belmer A, Beecher K, Ali SA, Chehrehasa F, Battle AR, Johnson
932 LR, Bartlett SE (2019) Contextual fear conditioning alter microglia number and
933 morphology in the rat dorsal hippocampus. Front Cell Neurosci 13:214.
934 Dash PK, Hochner B, Kandel ER (1990) Injection of the camp-responsive element into
935 the nucleus of *aplysia* sensory neurons blocks long-term facilitation. Nature
936 345:718-721.
937 Davis M, Astrachan DI (1978) Conditioned fear and startle magnitude: Effects of
938 different footshock or backshock intensities used in training. J Exp Psychol Anim
939 Behav Process 4:95-103.
940 Davis S, Vanhoutte P, Pages C, Caboche J, Laroche S (2000) The mapk/erk cascade
941 targets both elk-1 and camp response element-binding protein to control long-
942 term potentiation-dependent gene expression in the dentate gyrus in vivo. J
943 Neurosci 20:4563-4572.
944 de Oliveira Alvares L, Do-Monte FH (2021) Understanding the dynamic and destiny of
945 memories. Neurosci Biobehav Rev 125:592-607.
946 Detert JA, Kampa ND, Moyer JR, Jr. (2008) Differential effects of training intertrial
947 interval on acquisition of trace and long-delay fear conditioning in rats. Behav
948 Neurosci 122:1318-1327.
949 Di Benedetto B, Kallnik M, Weisenhorn DM, Falls WA, Wurst W, Holter SM (2009)
950 Activation of erk/mapk in the lateral amygdala of the mouse is required for

951 acquisition of a fear-potentiated startle response. Neuropsychopharmacology
952 34:356-366.
953 Do-Monte FH, Manzano-Nieves G, Quinones-Laracuente K, Ramos-Medina L, Quirk GJ
954 (2015) Revisiting the role of infralimbic cortex in fear extinction with optogenetics.
955 J Neurosci 35:3607-3615.
956 Ermentrout B (2002) Simulating, analyzing, and animating dynamical systems : A guide
957 to xppaut for researchers and students. Philadelphia: Society for Industrial and
958 Applied Mathematics.
959 Fernandez SM, Lewis MC, Pechenino AS, Harburger LL, Orr PT, Gresack JE, Schafe
960 GE, Frick KM (2008) Estradiol-induced enhancement of object memory
961 consolidation involves hippocampal extracellular signal-regulated kinase
962 activation and membrane-bound estrogen receptors. J Neurosci 28:8660-8667.
963 Flood JF, Jarvik ME, Bennett EL, Orme AE, Rosenzweig MR (1977) Protein synthesis
964 inhibition and memory for pole jump active avoidance and extinction. Pharmacol
965 Biochem Behav 7:71-77.
966 Genoux D, Haditsch U, Knobloch M, Michalon A, Storm D, Mansuy IM (2002) Protein
967 phosphatase 1 is a molecular constraint on learning and memory. Nature
968 418:970-975.
969 Goldsmith BA, Abrams TW (1991) Reversal of synaptic depression by serotonin at
970 aplysia sensory neuron synapses involves activation of adenylyl cyclase. Proc
971 Natl Acad Sci U S A 88:9021-9025.
972 Goode TD, Maren S (2014) Animal models of fear relapse. ILAR J 55:246-258.

973 Hawkins RD, Byrne JH (2015) Associative learning in invertebrates. Cold Spring Harb
974 Perspect Biol 7.
975 Holmes A, Quirk GJ (2010) Pharmacological facilitation of fear extinction and the search
976 for adjunct treatments for anxiety disorders--the case of yohimbine. Trends
977 Pharmacol Sci 31:2-7.
978 Hunsaker MR, Kesner RP (2008) Dissociations across the dorsal-ventral axis of ca3
979 and ca1 for encoding and retrieval of contextual and auditory-cued fear.
980 Neurobiol Learn Mem 89:61-69.
981 Impey S, Obrietan K, Wong ST, Poser S, Yano S, Wayman G, Deloulme JC, Chan G,
982 Storm DR (1998) Cross talk between erk and pka is required for ca^{2+} stimulation
983 of creb-dependent transcription and erk nuclear translocation. Neuron 21:869-
984 883.
985 Jiang L, Wang L, Yin Y, Huo M, Liu C, Zhou Q, Yu D, Xu L, Mao R (2019) Spaced
986 training enhances contextual fear memory via activating hippocampal 5-ht2a
987 receptors. Front Mol Neurosci 12:317.
988 Johansen JP, Cain CK, Ostroff LE, LeDoux JE (2011) Molecular mechanisms of fear
989 learning and memory. Cell 147:509-524.
990 Kandel ER (2001) The molecular biology of memory storage: A dialogue between genes
991 and synapses. Science 294:1030-1038.
992 Kheirbek MA, Drew LJ, Burghardt NS, Costantini DO, Tannenholz L, Ahmari SE, Zeng
993 H, Fenton AA, Hen R (2013) Differential control of learning and anxiety along the
994 dorsoventral axis of the dentate gyrus. Neuron 77:955-968.

995 Kida S (2012) A functional role for creb as a positive regulator of memory formation and
996 ltp. Exp Neurobiol 21:136-140.
997 Lauterborn JC, Palmer LC, Jia Y, Pham DT, Hou B, Wang W, Trieu BH, Cox CD,
998 Kantorovich S, Gall CM, Lynch G (2016) Chronic ampakine treatments stimulate
999 dendritic growth and promote learning in middle-aged rats. J Neurosci 36:1636-
1000 1646.
1001 Lee K, Holley SM, Shobe JL, Chong NC, Cepeda C, Levine MS, Masmanidis SC (2017)
1002 Parvalbumin interneurons modulate striatal output and enhance performance
1003 during associative learning. Neuron 93:1451-1463 e1454.
1004 Liu RY, Cleary LJ, Byrne JH (2011) The requirement for enhanced creb1 expression in
1005 consolidation of long-term synaptic facilitation and long-term excitability in
1006 sensory neurons of *aplysia*. J Neurosci 31:6871-6879.
1007 Liu X, Ramirez S, Pang PT, Puryear CB, Govindarajan A, Deisseroth K, Tonegawa S
1008 (2012) Optogenetic stimulation of a hippocampal engram activates fear memory
1009 recall. Nature 484:381-385.
1010 Lonsdorf TB et al. (2017) Don't fear 'fear conditioning': Methodological considerations
1011 for the design and analysis of studies on human fear acquisition, extinction, and
1012 return of fear. Neurosci Biobehav Rev 77:247-285.
1013 Lynch G, Cox CD, Gall CM (2014) Pharmacological enhancement of memory or
1014 cognition in normal subjects. Front Syst Neurosci 8:90.
1015 Lynch MA (2004) Long-term potentiation and memory. Physiol Rev 84:87-136.

1016 Malenka RC, Kauer JA, Perkel DJ, Mauk MD, Kelly PT, Nicoll RA, Waxham MN (1989)
1017 An essential role for postsynaptic calmodulin and protein kinase activity in long-
1018 term potentiation. Nature 340:554-557.
1019 Maren S (2005) Synaptic mechanisms of associative memory in the amygdala. Neuron
1020 47:783-786.
1021 Maren S, Phan KL, Liberzon I (2013) The contextual brain: Implications for fear
1022 conditioning, extinction and psychopathology. Nat Rev Neurosci 14:417-428.
1023 Martin KC, Michael D, Rose JC, Barad M, Casadio A, Zhu H, Kandel ER (1997) Map
1024 kinase translocates into the nucleus of the presynaptic cell and is required for
1025 long-term facilitation in *aplysia*. Neuron 18:899-912.
1026 Martin SJ, Grimwood PD, Morris RG (2000) Synaptic plasticity and memory: An
1027 evaluation of the hypothesis. Annu Rev Neurosci 23:649-711.
1028 Mast M, Blanchard RJ, Blanchard DC (1982) The relationship of freezing and response
1029 suppression in a cer situation. The Psychological Record 32:151.
1030 Mayes A, Montaldi D, Migo E (2007) Associative memory and the medial temporal
1031 lobes. Trends Cogn Sci 11:126-135.
1032 McDougal RA, Morse TM, Hines ML, Shepherd GM (2015) Modelview for modeldb:
1033 Online presentation of model structure. Neuroinformatics 13:459-470.
1034 McGaugh JL, Petrinovich LF (1965) Effects of drugs on learning and memory. Int Rev
1035 Neurobiol 8:139-196.
1036 Milner B, Squire LR, Kandel ER (1998) Cognitive neuroscience and the study of
1037 memory. Neuron 20:445-468.

1038 Morgan MA, LeDoux JE (1995) Differential contribution of dorsal and ventral medial
1039 prefrontal cortex to the acquisition and extinction of conditioned fear in rats.
1040 Behav Neurosci 109:681-688.
1041 Muller U, Carew TJ (1998) Serotonin induces temporally and mechanistically distinct
1042 phases of persistent pka activity in *aplysia* sensory neurons. Neuron 21:1423-
1043 1434.
1044 Nabavi S, Fox R, Proulx CD, Lin JY, Tsien RY, Malinow R (2014) Engineering a
1045 memory with ltd and ltp. Nature 511:348-352.
1046 Nakazawa K, Quirk MC, Chitwood RA, Watanabe M, Yeckel MF, Sun LD, Kato A, Carr
1047 CA, Johnston D, Wilson MA, Tonegawa S (2002) Requirement for hippocampal
1048 ca3 nmda receptors in associative memory recall. Science 297:211-218.
1049 Padilla-Coreano N, Do-Monte FH, Quirk GJ (2012) A time-dependent role of midline
1050 thalamic nuclei in the retrieval of fear memory. Neuropharmacology 62:457-463.
1051 Park S, Kramer EE, Mercaldo V, Rashid AJ, Insel N, Frankland PW, Josselyn SA (2016)
1052 Neuronal allocation to a hippocampal engram. Neuropsychopharmacology
1053 41:2987-2993.
1054 Paxinos G, Watson C (2014) Paxino's and watson's the rat brain in stereotaxic
1055 coordinates, Seventh edition. Edition. Amsterdam ; Boston: Elsevier/AP,
1056 Academic Press is an imprint of Elsevier.
1057 Philips GT, Tzvetkova EI, Carew TJ (2007) Transient mitogen-activated protein kinase
1058 activation is confined to a narrow temporal window required for the induction of
1059 two-trial long-term memory in *aplysia*. J Neurosci 27:13701-13705.

1060 Phillips RG, LeDoux JE (1992) Differential contribution of amygdala and hippocampus
1061 to cued and contextual fear conditioning. Behav Neurosci 106:274-285.
1062 Podlesnik CA, Kelley ME, Jimenez-Gomez C, Bouton ME (2017) Renewed behavior
1063 produced by context change and its implications for treatment maintenance: A
1064 review. J Appl Behav Anal 50:675-697.
1065 Quirk GJ, Mueller D (2008) Neural mechanisms of extinction learning and retrieval.
1066 Neuropsychopharmacology 33:56-72.
1067 Quirk GJ, Russo GK, Barron JL, Lebron K (2000) The role of ventromedial prefrontal
1068 cortex in the recovery of extinguished fear. J Neurosci 20:6225-6231.
1069 Radulovic J, Tronson NC (2010) Molecular specificity of multiple hippocampal
1070 processes governing fear extinction. Rev Neurosci 21:1-17.
1071 Raman M, McLaughlin K, Violato C, Rostom A, Allard JP, Coderre S (2010) Teaching in
1072 small portions dispersed over time enhances long-term knowledge retention.
1073 Med Teach 32:250-255.
1074 Restivo L, Tafi E, Ammassari-Teule M, Marie H (2009) Viral-mediated expression of a
1075 constitutively active form of creb in hippocampal neurons increases memory.
1076 Hippocampus 19:228-234.
1077 Roberson ED, Sweatt JD (1996) Transient activation of cyclic amp-dependent protein
1078 kinase during hippocampal long-term potentiation. The Journal of biological
1079 chemistry 271:30436-30441.
1080 Santini E, Muller RU, Quirk GJ (2001) Consolidation of extinction learning involves
1081 transfer from nmda-independent to nmda-dependent memory. J Neurosci
1082 21:9009-9017.

1083 Santini E, Ge H, Ren K, Pena de Ortiz S, Quirk GJ (2004) Consolidation of fear
1084 extinction requires protein synthesis in the medial prefrontal cortex. J Neurosci
1085 24:5704-5710.
1086 Schacher S, Castellucci VF, Kandel ER (1988) Camp evokes long-term facilitation in
1087 *aplysia* sensory neurons that requires new protein synthesis. Science 240:1667-
1088 1669.
1089 Schafe GE, LeDoux JE (2000) Memory consolidation of auditory pavlovian fear
1090 conditioning requires protein synthesis and protein kinase a in the amygdala. J
1091 Neurosci 20:RC96.
1092 Schafe GE, Atkins CM, Swank MW, Bauer EP, Sweatt JD, LeDoux JE (2000) Activation
1093 of erk/map kinase in the amygdala is required for memory consolidation of
1094 pavlovian fear conditioning. J Neurosci 20:8177-8187.
1095 Scharf MT, Woo NH, Lattal KM, Young JZ, Nguyen PV, Abel T (2002) Protein synthesis
1096 is required for the enhancement of long-term potentiation and long-term memory
1097 by spaced training. J Neurophysiol 87:2770-2777.
1098 Selden NR, Everitt BJ, Jarrard LE, Robbins TW (1991) Complementary roles for the
1099 amygdala and hippocampus in aversive conditioning to explicit and contextual
1100 cues. Neuroscience 42:335-350.
1101 Sharif S, Guirguis A, Fergus S, Schifano F (2021) The use and impact of cognitive
1102 enhancers among university students: A systematic review. Brain Sci 11.
1103 Sharma SK, Carew TJ (2004) The roles of mapk cascades in synaptic plasticity and
1104 memory in *aplysia*: Facilitatory effects and inhibitory constraints. Learn Mem
1105 11:373-378.

1106 Sharma SK, Sherff CM, Shobe J, Bagnall MW, Sutton MA, Carew TJ (2003) Differential
1107 role of mitogen-activated protein kinase in three distinct phases of memory for
1108 sensitization in *aplysia*. J Neurosci 23:3899-3907.
1109 Sindreu CB, Scheiner ZS, Storm DR (2007) Ca2+ -stimulated adenylyl cyclases
1110 regulate erk-dependent activation of msk1 during fear conditioning. Neuron
1111 53:79-89.
1112 Smolen P, Zhang Y, Byrne JH (2016) The right time to learn: Mechanisms and
1113 optimization of spaced learning. Nat Rev Neurosci 17:77-88.
1114 Smolen P, Baxter DA, Byrne JH (2020) Comparing theories for the maintenance of late
1115 ltp and long-term memory: Computational analysis of the roles of kinase
1116 feedback pathways and synaptic reactivation. Front Comput Neurosci
1117 14:569349.
1118 Sotres-Bayon F, Sierra-Mercado D, Pardilla-Delgado E, Quirk GJ (2012) Gating of fear
1119 in prelimbic cortex by hippocampal and amygdala inputs. Neuron 76:804-812.
1120 Szapiro G, Vianna MR, McGaugh JL, Medina JH, Izquierdo I (2003) The role of nmda
1121 glutamate receptors, pka, mapk, and camkii in the hippocampus in extinction of
1122 conditioned fear. Hippocampus 13:53-58.
1123 Tronson NC, Schrick C, Fischer A, Sananbenesi F, Pages G, Pouyssegur J, Radulovic
1124 J (2008) Regulatory mechanisms of fear extinction and depression-like behavior.
1125 Neuropsychopharmacology 33:1570-1583.
1126 Vázquez SI, Vázquez A, Peña de Ortiz S (2000) Different hippocampal activity profiles
1127 for pka and pkc in spatial discrimination learning. Behavioral Neuroscience
1128 114:1109-1118.

1129 Verkoeijen PP, Rikers RM, Schmidt HG (2005) Limitations to the spacing effect:
1130 Demonstration of an inverted u-shaped relationship between interrepetition
1131 spacing and free recall. Exp Psychol 52:257-263.
1132 Wang S, Sheng T, Ren S, Tian T, Lu W (2016) Distinct roles of pkcı/λ and pkmζ in the
1133 initiation and maintenance of hippocampal long-term potentiation and memory.
1134 Cell Rep 16:1954-1961.
1135 Wang Y, Zhu G, Briz V, Hsu YT, Bi X, Baudry M (2014) A molecular brake controls the
1136 magnitude of long-term potentiation. Nature communications 5:3051.
1137 Woods AM, Bouton ME (2008) Immediate extinction causes a less durable loss of
1138 performance than delayed extinction following either fear or appetitive
1139 conditioning. Learn Mem 15:909-920.
1140 Zhang Y, Smolen PD, Cleary LJ, Byrne JH (2021) Quantitative description of the
1141 interactions among kinase cascades underlying long-term plasticity of *aplysia*
1142 sensory neurons. Scientific reports 11:14931.
1143 Zhang Y, Liu RY, Heberton GA, Smolen P, Baxter DA, Cleary LJ, Byrne JH (2011)
1144 Computational design of enhanced learning protocols. Nat Neurosci 15:294-297.
1145
1146
1147
1148
1149
1150
1151
1152